AD-A254 436

PAGE

Form Approved
OMB No. 0704-0188

1. AGENCY USE ONLY (Leave blank)	2. REPORT DATE	3. REPORT TYPE AND DATES COVERED
	1992	THESIS

4. TITLE AND SUBTITLE

The Role of Latent Heat Release in Explosive Cyclogenesis

5. FUNDING NUMBERS

6. AUTHOR(S)

Donald M. Rinderknecht, Captain

7. PERFORMING ORGANIZATION NAME(S) AND ADDRESS(ES)

AFIT Student Attending: Saint Louis University

8. PERFORMING ORGANIZATION REPORT NUMBER

AFIT/CI/CIA-92-052

9. SPONSORING/MONITORING AGENCY NAME(S) AND ADDRESS(ES)

AFIT/CI
Wright-Patterson AFB OH 45433-6583

10. SPONSORING/MONITORING AGENCY REPORT NUMBER

DTIC
ELECTE
AUG 31 1992
S C D

11. SUPPLEMENTARY NOTES

12a. DISTRIBUTION/AVAILABILITY STATEMENT

Approved for Public Release IAW 190-1
Distributed Unlimited
ERNEST A. HAYGOOD, Captain, USAF
Executive Officer

12b. DISTRIBUTION CODE

13. ABSTRACT *(Maximum 200 words)*

92-23901

012200   78p.

14. SUBJECT TERMS

15. NUMBER OF PAGES

76

16. PRICE CODE

17. SECURITY CLASSIFICATION OF REPORT	18. SECURITY CLASSIFICATION OF THIS PAGE	19. SECURITY CLASSIFICATION OF ABSTRACT	20. LIMITATION OF ABSTRACT

THE ROLE OF LATENT HEAT RELEASE IN EXPLOSIVE CYCLOGENESIS

Donald Matthew Rinderknecht, B.S.

A Digest Presented to the Faculty of the Graduate School
of Saint Louis University in Partial Fulfillment of
the Requirements for the Degree of
Master of Science (Research)

1992

Digest

Extratropical cyclones and their attendant fronts are the primary cause of day to day weather changes at any given location in middle and higher latitudes. Storms that deepen at least 24 mb in a period of 24 hours or less are rapid developing storms. This research attempts to analyze the role of latent heating in explosive cyclogenesis, using the Sutcliffe Development Equation (SDE). The SDE describes cyclone development in terms of absolute vorticity advection, thickness advection, stability, and latent heating. The basic premise to be tested is that latent heating, including stable and convective components, plays a significant role in the rapid development of extratropical cyclones.

The Sutcliffe Equation Analysis Model (SEAM), developed to study these storms, uses a grid of 27 points (x axis) by 18 points (y axis) with a spacing of 190.5 km. Vertical resolution in the SEAM consists of 19 levels from 1000 mb to 100 mb in 50 mb increments. The moael atmosphere extends to 100 mb to accommodate moisture convergence and subordinate parameters needed to calculate latent heating, which is parameterized into two basic types; stable and convective latent heat release. Stable latent heat release (SLHR) is a large scale effect while convective latent heat release (CLHR) is a sub-grid scale effect.

Analysis of results show that CLHR values were virtually non-existent in the normal case and very small in the bomb case. Comparison of Sutcliffe values and storm tracks show that areas of positive values downstream of the surface center indicate movement of either type of storm. The explosive storm followed along the Sutcliffe value ridge, while the normal storm moved perpendicular to the ridge. These preliminary results indicate that latent heat release is important in rapid development.

THE ROLE OF LATENT HEAT RELEASE IN EXPLOSIVE CYCLOGENESIS

Donald Matthew Rinderknecht, B.S.

A Thesis Presented to the Faculty of the Graduate School
of Saint Louis University in Partial Fulfillment of
the Requirements for the Degree of
Master of Science (Research)

1992

COMMITTEE IN CHARGE OF CANDIDACY:

Professor James T. Moore,
　　　　Chairperson and Advisor

Professor Frank Y. J. Lin

Professor G. V. Rao

For Penney.

(Is it MY turn to do the dishes?)

Acknowledgements

Table of Contents

List of Figures

Chapter 1: Introduction

1.1 Importance of Explosive Cyclogenesis

Extratropical cyclones and their attendant warm, cold and occluded fronts are the primary cause of day to day weather changes at any given location in middle and higher latitudes. As a result, cyclogenesis has been a significant area of study over at least the past 150 years (Uccellini, 1988). A significant subset of extratropical cyclones are those that develop considerably faster than the normal cyclone in a period of 24 hours or less. Rapid, or explosive cyclogenesis is defined as a deepening of central storm pressure by 1 mb per hour for a period of 24 hours, with correction for change in latitude (Sanders and Gyakum, 1980). Storms that develop at a slower rate than 24 mb in 24 hours are considered non-explosive or, for this study, normal cyclogenesis.

Statistical studies (Roebber, 1984, 1989; Sanders and Gyakum, 1980) show that explosive cyclogenesis is primarily a maritime event, however, this does not mean that continental rapid cyclogenesis is insignificant. Roebber (1989) states that continental storms show a distinct fundamental difference in character from maritime events, justifying the study of continental explosive cyclogenesis exclusive of maritime events, despite the relative infrequency of such continental events. Another factor in favor of studying continental storms in particular is that data density and availability are maximized over continental areas as opposed to the sparsity of data in oceanic areas.

Recent forecast techniques fall short in the prediction of explosive cyclogenesis. As described by Sanders (1987), the global spectral model (GLBL) and the Nested-Grid Model (NGM) perform relatively poorly in continental cases. One must take into ac-

count, of course, that these cases are small in number. In the study of numerical models, and forecasting in general, a false alarm is when an event was forecast to occur but in fact did not occur. Sanders (1987) defined the false alarm rate (FAR) as the ratio of false alarms (FA) to the number of accurate forecasts or hits (H) and false alarms combined. Mathematically this can be stated as; FAR = FA / (FA + H). From this equation it is clear that a higher number of hits compared to false alarms will lower the false alarm rate. Sanders' statistics show that the NGM had a FAR of 0.71, while the GLBL had a FAR of 0.80 for his study of cyclones from September 1986 through April 1987. The performance of the models as illustrated by Sanders is justification for continued study of continental explosive cyclogenesis.

Undoubtedly, there are numerous complex mechanisms involved in the generation of cyclogenesis in general, and rapid cyclogenesis in particular. This research focuses specifically on latent heat release as related to explosive cyclogenesis. Early in the history of study of these issues (Uccellini, 1980), latent heat release was an important factor in the thermal theory of cyclones. Roebber (1984) as well as others, have referred to latent heat release as possibly having a significant influence in the development of extratropical cyclones.

Having chosen latent heat release for more detailed study, a tool for analysis of this parameter is needed. The Sutcliffe Development Equation (SDE), as described by Petterssen (1956) and modified based upon subsequent research, describes cyclone development in terms of absolute vorticity advection, thickness advection, stability, and latent heating. To the authors knowledge, the SDE has not been applied as an analysis tool.

1.2 Statement of Thesis

In a limited case comparison of continental extratropical cyclones analyzed under the scrutiny of the SDE, this research will attempt to detect and analyze the role of latent heating in explosive cyclogenesis. The basic premise to be tested is that latent heating, including stable and convective components, plays a significant role in the rapid development of extratropical cyclones. Towards this end, the terms of the SDE will be analyzed on a combined and individual basis in order to understand any possible synergism between the respective terms, the domination of any specific term, and the horizontal spatial distribution of these terms. In addition, the resultant value of the SDE will be analyzed in light of the contribution of the latent heating term in an effort to aid in the understanding of explosive continental cyclogenesis. The SDE will be applied to a rapidly intensifying cyclone event and a modest cyclone event to compare the significance of latent heating in the development of the respective storms.

Chapter 2: Review of Literature

2.1 A Brief History of Cyclogenesis

Cyclogenesis has been a focus of study since the nineteenth century (Uccellini, 1988). Cyclogenesis is defined as the development of cyclonic circulation where none previously existed, or an increase in the strength of cyclonic flow that is already present. This is often seen as an increase in wave-like disturbances on the polar front. Initially, latent heat release was thought to be the primary cause of cyclogenesis. By the mid-twentieth century (Fig. 2-1) attention turned to dynamical processes to explain cyclogenesis, with baroclinic instability as the primary focus.

Baroclinic instability is related to the distortion of the isotherms on a constant pressure surface, causing changes in kinetic energy. Kinetic energy is directly proportional to the strength of the cyclonic disturbance. In order for development to take place due to baroclinic instability, a direct thermal circulation must exist. In the meridional plane (Fig. 2-2) the isentropes slope downward into the warm air.

On the synoptic scale, isentropic surfaces act as material surfaces (Moore, 1987) to air motions. In the Northern Hemisphere westerlies, if the trajectories are sloped less than the isentropes (Fig. 2-2b), in the cold air advection on the west side of the trough the cold air is sinking, while in the warm air advection on the east side of the trough, the warm air is rising. This direct thermal circulation results in development. If the slope of the trajectories is greater than the slope of the isentropes (Fig. 2-2a), as is the case with shorter baroclinic waves, the thermal field becomes weaker and the wave dissipates (Wallace and Hobbs, 1977).

4

DYNAMIC PROCESSES EMERGE

POLAR FRONT CYCLONE MODEL DEVELOPED BY BERGEN SCHOOL

SYNOPTIC ANALYSES RAISE QUESTIONS CONCERNING VALIDITY OF THERMAL THEORY

REQUIREMENT FOR UPPER LEVEL DIVERGENCE ESTABLISHED

1900 V. BJERKNES
HANN MARGULES

"THERMAL THEORY" OF CYCLONES DEVELOPED: CYCLONES DRIVEN PRIMARILY BY LATENT HEAT RELEASE

LOOMIS

1920
DINES
SHERHAG

TROUGH-RIDGE PATTERN RELATED TO VERTICAL PROFILE OF DIVERGENCE

FERREL

1800's ESPY

J. BJERKNES HOLMBOE 1940

BAROCLINIC INSTABILITY THEORY AND "DEVELOPMENT EQUATIONS" DERIVED

EMANUEL ROTUNNO

CHARNEY
EADY   SUTCLIFFE
PETTERSSEN

RAPID CYCLOGENESIS IN EXTRATROPICAL REGIONS COMPARED TO HURRICANES

GYAKUM
1980
RASMUSSEN

PALMEN, NEWTON, RIEHL

ELIASSEN   1950

SYNOPTIC ANALYSES FLOURISH USING UPPER AIR DATA

KLEINSCHMIDT, REED
DANIELSEN

JOHNSON

Q. G. THEORY EMERGES

1960

1970   DANARD

ROLE OF STRATOSPHERIC EXTRUSIONS EXPLORED

LATENT HEAT RELEASE SHOWN TO BE IMPORTANT FOR RAPID SPIN-UP OF CYCLONES

LATENT HEATING REQUIRED FOR NUMERICAL MODELS TO SIMULATE CYCLOGENESIS

NUMERICAL MODELS DEVELOPED AND APPLIED TO WEATHER FORECASTING

Figure 2-1. Summary of significant developments in the study of cyclogenesis from the 1800s to the 1980s (after Uccellini, 1988).
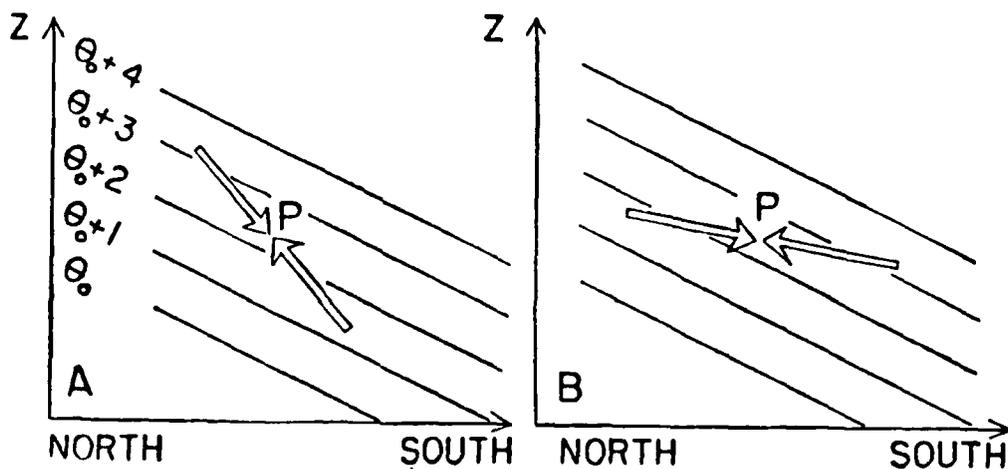
Figure 2-2. Baroclinic Instability. A meridional section depicting displacement of air parcels (arrows) in relation to potential isotherms (thin lines). A - short wavelength; B - medium wavelength (after Petterssen, 1956).

5

This emphasis of baroclinic instability seemed to dominate the explanations of cyclogenesis since the 1940s (Uccellini, 1988). However, some prominent synopticians including Petterssen, Sutcliffe, Palmen, and Newton, still recognized latent heat release as a significant factor. The fact that early numerical weather prediction models were not able to simulate explosive or rapid cyclogenesis brought renewed attention to the effects of latent heat release (Uccellini, 1988). Research in recent years has indeed shown that the release of latent heat is a significant process in cyclogenesis (Dare et al., 1985; Rao, 1972; Reed et al., 1988; Smith et al., 1984; Smith and Tsou, 1985). The debate on the influence of latent heating as opposed to dynamical processes in cyclogenesis still continues and will be discussed further in section 2.4.

2.2 Climatology of Explosive Cyclogenesis

As previously discussed, a cyclone is considered explosive if the central pressure deepens at a rate of at least 24 mb in 24 hours, or one Bergeron (Sanders and Gyakum, 1980). Due to the rapid development of this type of cyclone they are often unexpected by forecasters, potentially resulting in property damage, possible injury or loss of life that could be avoided with advance warning. This fact alone could justify extensive research into explosive cyclogenesis, however, there are more fundamental reasons for continued research.

Study of rapid cyclogenesis was originally inspired by the fact that numerical modeling efforts were unable to accurately predict storms that developed explosively (Sanders and Gyakum, 1980). Apparently, the models do not adequately parameterize the critical process or processes that are responsible for rapid cyclogenesis. Particularly interesting is that a majority of the strongest cyclones develop rapidly for some peri-

od of their existence (Sanders and Gyakum, 1980; Roebber,1984). Generally speaking then, the strongest extratropical cyclones are a result of explosive cyclogenesis and are poorly handled by current numerical models -- the primary tool of the operational forecaster.

A majority of research in the explosive development arena has been specifically related to oceanic cyclogenesis. This is primarily due to the relative high frequency of these storms (Sanders and Gyakum, 1980). Statistical analysis by Roebber (1984, 1989) has confirmed that oceanic rapid development is more common than continental storms by a vast margin (Fig. 2-3) but, more importantly, that developmental processes of oceanic storms are of a different nature than the storms over land. The physical mechanisms responsible for the distinction between oceanic and continental explosive cyclogenesis is open to discussion. Identification of specific processes responsible for rapid cyclogenesis could theoretically improve forecasts enough to allow for adequate advanced warning of these strong storms.

2.3 The Sutcliffe Development Theory

As noted in Fig. 2-1, Sutcliffe (1939, 1947) and Sutcliffe and Forsdyke (1950) derived a development equation for quantifying the rate of cyclone development to aid in understanding and forecasting of extratropical cyclones. The SDE is based upon the theory that typical cyclogenesis consists of an imbalance between convergence in lower levels and divergence in upper levels. This imbalance can be identified as a difference in horizontal acceleration between the surface and upper level and would be an indicator of development (Sutcliffe, 1939, 1947). Sutcliffe uses convergence, which is proportional to the rate of production of absolute vorticity, as a measure of the rate of
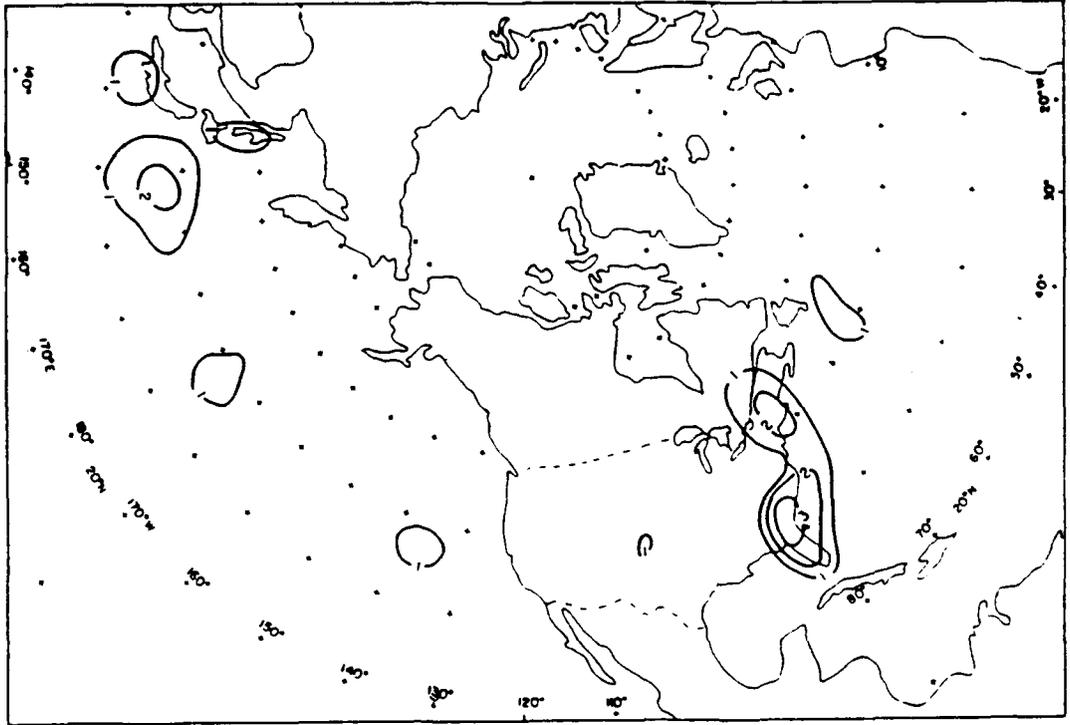
Figure 2-3. Geographic distribution of explosive cyclones (after Roebber, 1984).

8

development. Horizontal shear normally increases with height, which increases divergence relative to the surface, while at stratospheric heights, horizontal shear decreases with height (Sutcliffe, 1947). Development is dependent upon vertical wind shear, with the most rapid development being in areas of strongest vertical wind shear and horizontal temperature gradient. In general application, Sutcliffe (1947) expected to find that results from data at 1000 mb and 500 mb would be a reasonable approximation compared to results using the entire atmospheric column. The SDE, as described by Petterssen (1956), is formulated as follows:

$$\frac{\partial \zeta_{1000}}{\partial t} = -\vec{V}_{500} \cdot \nabla \, \eta_{500} - \frac{R_d}{f} \, \nabla^2 \left[\frac{1}{R_d} A_T + S + H \right] \qquad (1)$$

(See Appendix A for definition of symbols.) The terms of the SDE include the absolute geostrophic vorticity advection at 500 mb, and the Laplacian of each of the three remaining terms, including thickness advection:

$$A_T = - \overline{\vec{V}_{500} \cdot \nabla(\Delta \Phi)} \qquad (2)$$

stability:

$$S = \left(\ln \frac{1000}{500} \right) \overline{\frac{\omega}{\rho g} (\Gamma_D - \gamma)} \qquad (3)$$

and diabatic heating:

$$H = \left(\ln \frac{1000}{500} \right) \overline{\frac{1}{c_p} \frac{dQ}{dt}} \qquad (4)$$

The overbar in these terms indicates an averaged value between 1000 mb and 500 mb. Detailed properties parameterizations and calculations of each term are discussed in Chapter 3. Generally speaking, however, the vorticity and thickness terms tend to dominate the equation while the stability and diabatic terms are smaller, but still important in their contribution to the rate of development.

2.4 Aspects of Latent Heating in Cyclogenesis

There is no single numerical value denoting the effect of latent heat release in normal or explosive cyclogenesis. The impact of latent heating is expected to vary by geographical area and season, on a case by case basis (Reed et al., 1988). Latent heating is parameterized into two basic types; stable and convective latent heat release. Stable latent heating is considered a large scale effect while convective latent heating is considered to be a small scale effect. In numerical models on a scale larger than meso-scale, the convective latent heating is sub-grid scale. This complicates parameterization considerably and will be discussed further in Chapter 3.

Smith, Dare and Lin (1984) compared latent heat and dry dynamical processes. Results showed that dry dynamical processes were important early in cyclone development. The period of maximum development occurred after latent heating had subsided, indicating that the latent heat release is a precursor to rapid development. At the time of maximum development latent heating accounted for up to 50% of the total vertical motion. Similarly, Macdonald and Reiter (1988) found that stable latent heat release increased dramatically between the incipient and explosive stages of rapidly developing cyclones. This is in contrast to their results for normal cyclones which showed much less latent heating as a whole during the life of the storm and smaller

changes in heating between different phases of storm development. In the case of convective latent heat release, they found that the maximum amount of latent heat release occurs in the incipient stage with dramatically less heating in the subsequent stages. Maximum convective latent heating in the normal cyclone was found to occur in the intermediate phase. Conceivably then, heavy convective precipitation could be a triggering mechanism for explosive cyclogenesis.

Dare et al. (1985) found that although the basic development and propagation of their case study was dominated by dry dynamical processes, moist physics intensified the event. They found that stable latent heating was more important in influencing cyclone development than convective latent heating.

In a study of diabatic forcing, Smith and Tsou (1985) found that latent heat release was significant to development but was hidden in area averaged statistics due to the fact that the area affected by latent heat release was of a limited horizontal extent. Similarly, Manabe (1956) found that latent heating from small scale condensation was, in effect, filtered out of the large scale analysis. Smith and Tsou (1985) found, with regard to height tendency pattern accuracy, model runs including latent heating were significantly superior to those without latent heating included. Latent heat release was also found to work in concert with vorticity advection and thermal advection during explosive development, lending credence to the SDE.

In two cases of explosive cyclogenesis in the North Atlantic, Reed et al. (1988) found latent heating to be responsible for 40% to 50% of the deepening of these storms. For Reed, this fact reaffirmed the importance of moist processes in cyclogenesis.

Chapter 3: Data Processing and Computational Procedures

3.1 Sutcliffe Equation Analysis Model Description

An analysis model has been developed to study explosive cyclogenesis using the SDE. The Sutcliffe Equation Analysis Model (SEAM) uses a grid of 27 points (x axis) by 18 points (y axis) with a spacing of 190.5 km. Vertical resolution in the SEAM consists of 19 levels from 1000 mb to 100 mb in 50 mb increments. Consequently, when layers are required for analysis, there are 18 layers of 50 mb thickness available for use. The model atmosphere extends to 100 mb to accommodate moisture convergence and subordinate parameters needed to calculate latent heating. The SDE (1) uses data at and below the level of non-divergence, assumed to be 500 mb in the SEAM. For simplification of calculation, the 1000 mb level, the lowest level in the model, is assumed to be the surface at all grid points. The area of interest is centered on the United States.

3.2 Data Description and Preliminary Processing

The SEAM utilizes standard upper air sounding data for the continental United States as well as limited Canadian and Mexican stations. These data, as opposed to special experiment data, are chosen for use because of standardization and widespread availability among operational weather organizations.

Both mandatory and significant levels of upper air soundings from 900 mb to 100 mb are ingested into the SEAM, including values of temperature, dewpoint, wind, and heights. To complete the data required for the model, values for 950 mb and 1000

mb are calculated using a linear extrapolation technique. Extrapolated temperature and dew point values are based upon a 100 mb layer while extrapolated velocities are based upon a 50 mb layer. Height values are extrapolated to these higher pressure levels using the hypsometric equation. All data values are then assigned to grid points using a Barnes (1973) analysis. After the data has been prepared, adjusted kinematic omega values (O'Brien, 1970) are calculated for use in the latent heating and stability routines. At this point all necessary data are available for calculating the SDE.

3.3 Sutcliffe Development Equation Calculations

The individual terms of the SEAM are described in detail in this section including numerical parameterizations. The general influence and effect of each term on the development process will also be addressed. Specific meteorological effects, influences and interactions of the terms as applicable to the case studies are discussed in chapters 4 and 5.

3.3.1 Absolute Vorticity Advection

Calculation of the absolute vorticity advection term is relatively common in numerical weather analysis. Petterssen (1956) notes that an upper level trough with positive vorticity advection (PVA) ahead of it overtaking a frontal system in the lower troposphere is one of the most reliable indicators of cyclogenesis at sea level. Under the constraints of the quasigeostrophic theory the absolute vorticity advection term is calculated using geostrophic components of the wind at the level of non-divergence, previously defined to be 500 mb for this study.

The components of the geostrophic wind are calculated by standard methods. The u and v components are written as:

$$u_g = -\frac{1}{f}\left(\frac{\partial \Phi}{\partial y}\right) \qquad (5a)$$

$$v_g = \frac{1}{f}\left(\frac{\partial \Phi}{\partial x}\right) \qquad (5b)$$

Absolute vorticity is the sum of two components; relative vorticity and the Coriolis parameter. The Coriolis parameter is latitude dependent while relative vorticity is calculated using components of the geostrophic wind as follows:

$$\zeta_g = \frac{\partial v_g}{\partial x} - \frac{\partial u_g}{\partial y} = \frac{\nabla^2 \Phi}{f} \qquad (6)$$

The absolute geostrophic vorticity is then advected using the geostrophic wind at 500 mb resulting in:

$$-\vec{V}_{500} \cdot \nabla \eta_{500} = -u_g \frac{\partial \eta_g}{\partial x} - v_g \frac{\partial \eta_g}{\partial y} \qquad (7)$$

which is identifiable as the absolute geostrophic vorticity advection term from (1). Despite the fact that upper level troughs and associated vorticity are commonplace, development at low levels is not as common (Petterssen, 1956). This indicates that although it is a primary consideration, vorticity advection does not solely initiate low level cyclogenesis. Thermodynamic contributions must also be considered.

3.3.2 Laplacian of Thickness Advection

The second term of the SDE is the Laplacian of the 1000 mb to 500 mb thickness advection. Since the Laplacian is key to the remaining terms of the SDE, it will be detailed in this section. Petterssen (1956) illuminates the importance of the thickness term. Primarily, thickness advection influences the movement of the cyclone. Once the thermal patterns have been changed because of the circulation, the thickness advection contributes positively to development of the cyclone. Note that the shape and nonlinear characteristics of the feature is the important factor when considering Laplacians. The distortion of the thickness advection will clearly effect the Laplacian of this parameter. Figure 3-1 is a sample of the thickness advection prior to the Laplacian operation. Note the thickness advection ridge from Michigan to Louisiana as well as the trough from the Dakotas into Iowa. After the Laplacian operator is applied the ridges become maxima and troughs minima, as seen by comparing Fig. 3-1 and 3-2.

The first step is to calculate the value of the thickness. This is done by taking the difference between the geopotential at 500 mb and at 1000 mb. This value is then advected using a density weighted average wind from 1000 mb to 500 mb as described by (8).

$$-\vec{V} \cdot \nabla(\Delta\Phi) = -\bar{u}\,\frac{\partial(\Delta\Phi)}{\partial x} - \bar{v}\,\frac{\partial(\Delta\Phi)}{\partial y} \qquad (8)$$

Thickness advection values are extrapolated back to the edge of the grid using a simple linear extrapolation scheme. The Laplacian is then taken using the Schaefer (1977) method. This method provides for smoother and theoretically more accurate results.

THICKNESS ADVECTION (RAW VALUE) (10**-3 m/s)
12-15-1987 12 UTC
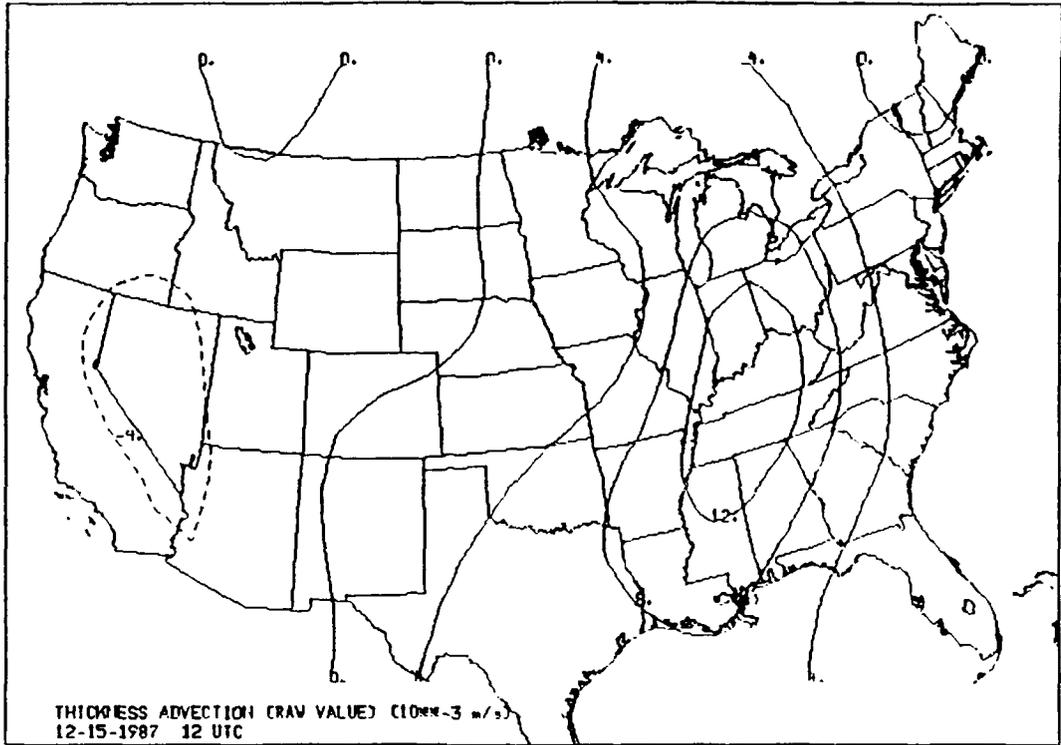
Figure 3-1.   Sample of thickness advection.

THICKNESS ADVECTION TERM (x10**-10 1/s**2)
12-15-1987 12 UTC
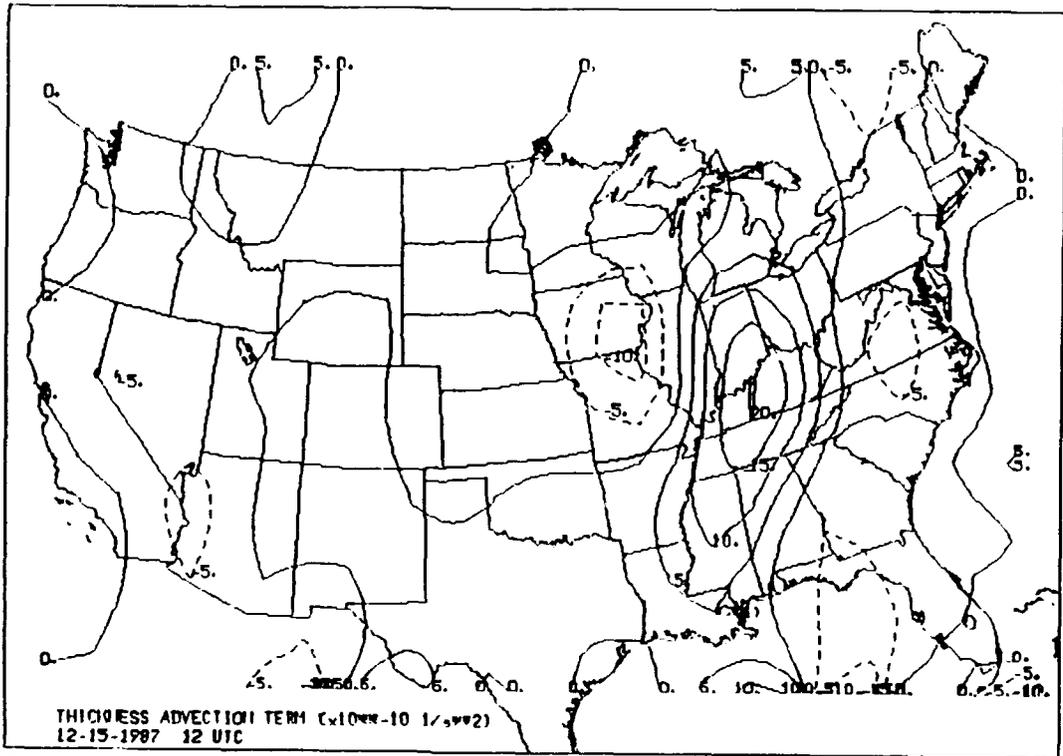
Figure 3-2.   Sample of the Laplacian of thickness advection.

The formula for the Schaefer Laplacian is (9):

$$\nabla^2 = \frac{1}{5\delta^2} \{ 8 \ [F(i+1, j)+F(i-1, j)+F(i, j+1)+F(i, j-1)]$$
$$- \frac{3}{2} \ [F(i+1, j+1)+F(i+1, j-1)+F(i-1, j-1)+F(i-1, j+1)] \tag{9}$$
$$- 26 \ F(i, j) \}$$

After taking the Laplacian the linear extrapolation technique is again used. This will undoubtedly cause some concern as to the accuracy of values near the edge of the grid. Due to the nature of storms being in the center areas of the grid this should cause no significant errors to data of interest. Finally, to complete calculation of the term, the values are divided by the negative of the Coriolis parameter.

3.3.3 The Laplacian of Stability

The third term in the SDE is the stability term. This term represents effects of adiabatic temperature changes (Petterssen, 1956). As seen in (3), the stability term depends on vertical motion, density, and the difference between the adiabatic lapse rate and the environmental lapse rate. Calculation of vertical motion has been discussed previously. The adiabatic lapse rate may be either the moist or dry rate depending upon the relative humidity (RH).

The stability term is significant in that it acts as a brake to cyclogenesis due to adiabatic cooling in areas of static stability when there is upward vertical motion below the level of non-divergence. However, in moist conditions when the environmental lapse rate exceeds the moist adiabatic lapse rate, the stability term contributes to development. Note that this property of the stability term has a more significant effect once the cloud system has been developed and moist conditions abound. In areas of

stable conditions and downward vertical motion this term contributes positively toward development at sea level as well. The primary effect of this term, however, is to work against development (Petterssen, 1956).

The stability term is averaged from 1000 mb to 500 mb. The first step in the parameterization includes validation of dew point values. The dew point is checked to be less than or equal to the temperature at a given level. Above 300 mb, for missing dew point values, the dew point is assigned to be 30 degrees less than the temperature at that level. The environmental lapse rate is calculated for each 50 mb layer using a simple difference. These values are then averaged from 1000 mb to 500 mb for use in the calculation of the stability term. The 1000 mb to 500 mb average requires a minimum of two levels with values for environmental lapse rate or the values are assigned as missing.

The moist and dry adiabatic lapse rates are calculated based upon a critical RH value of 0.80. This value is considered to be the threshold for saturation and was chosen for consistency with latent heating calculations. Layers of 50 mb in the model with an average RH < 0.80 are assigned the dry adiabatic lapse rate of 0.0098 K/m. Conversely for layers with an average RH $\geq$ 0.80 the moist adiabatic lapse rate is calculated using the method described in Hess (1959). Values for vertical motion, RH, static stability and virtual temperature are averaged for each layer and also in the vertical at each grid point for the model atmosphere. The vertical column averages for each grid point are calculated for the environmental lapse rate as well.

The static stability is calculated following the method presented by Hirschberg and Fritsch (1991). This parameterization consists of separate calculations of static

stability for both moist (S_m) and dry (S_d) conditions based upon the critical RH value of 0.80. The static stability values are calculated individually using (10a) and (10b) for each layer in the model.

$$S_d = -\frac{T_v}{\Theta_v}\frac{\partial\Theta_v}{\partial p} \quad \text{for} \quad RH<0.8 \quad \text{or} \quad \omega>0 \qquad \text{(10a)}$$

$$S_m = -\frac{T_v}{\Theta_e}\frac{\partial\Theta_e}{\partial p} \quad \text{for} \quad RH\geq0.8 \quad \text{and} \quad \omega<0 \qquad \text{(10b)}$$

These moist and dry static stability values are then averaged for a given grid point column, comprising the adjusted static stability parameter (S_a). Therefore, S_a consists of contributions from both moist and dry conditions. The calculation of static stability differs from that presented in (3). Static stability can be modified using Holton (1979) resulting in:

$$S_a = \frac{1}{\rho g}(\Gamma_D - \gamma) \qquad \text{(10c)}$$

which, when substituted into (3) defines the SEAM stability term as:

$$S = \left(\ln\frac{1000}{500}\right)\overline{\omega S_a} \qquad \text{(11)}$$

3.3.4 The Laplacian of Latent Heating

The fourth and final term in the SDE is the Laplacian of latent heating. Latent heating, as parameterized by Kuo (1965, 1974), Krishnamurti and Moxim (1971),

Krishnamurti et al. (1973), Edmon and Vincent (1976) and later modified by Smith, Dare and Lin (1984), consists of contributions from both convective and stable latent heating. The scheme developed by Kuo is the primary basis for the development of the convective latent heating in the SEAM, while Krishnamurti and Moxim (1971) and Edmon and Vincent (1976) are the main impetus for parameterization of the stable latent heat release (SLHR). Arguments concerning the advantages and disadvantages of this cumulus parameterization scheme are outside the scope of this document. However, methods have been chosen that have been generally accepted by researchers as published in the journals.

Generally speaking, deep convection is the source of convective latent heating. Considering the fact that convection is on a much smaller scale than the grid of the SDE, parameterization of this source of energy is relatively complex. In contrast, stable latent heat release is on a larger scale that is resolvable by the grid used in the SEAM. Consequently, the parameterization is much simpler for stable latent heat release as opposed to the convective contribution. Preprocessing of data is completed as described in section 3.2 before calculation of stable and convective latent heating.

In order for the release of stable latent heating to exist, three basic conditions must be met for each appropriate layer or grid point. Saturation must exist, as represented by a critical relative humidity value, and upward vertical motion must be present Vertical motion is calculated using a kinematic approach as presented by O'Brien (1970) and recommended by Smith and Lin (1978). Finally, there must be vertical moisture convergence in the pertinent layer. In the SEAM, stable latent heating is calculated for each 50 mb layer at each grid point. These values are also averaged for the 1000 mb to 500 mb layer for subsequent computations. Stable latent heating is

represented by (12).

$$SLHR = -\frac{L\omega}{c_p} \frac{\partial q_s}{\partial p} \tag{12}$$

When the above mentioned criteria are met, this equation results in a value for stable latent heating. Vertical moisture convergence for the layer is defined as the difference in saturation mixing ratio between the top and bottom of the layer. The saturation requirement is not directly represented. Saturation is based upon the average RH in the layer. RH and other vital parameters are calculated using the FORTRAN routines presented by Doswell et al. (1982). As previously discussed, the critical value of RH is 0.80 in the SEAM as recommended by Rao and Hassebrock (1972), Krishnamurti and Moxim (1971), and Edmon and Vincent (1976). In addition, the value for the rate of latent heating is a function of temperature. For temperatures above -20 C latent heat of vaporization is used, otherwise the latent heat of sublimation is used for the calculation of SLHR.

Latent heating from convective processes is considerably complex. Convective latent heating in the SDE is due to deep convection. Because of the small areal extent of deep convection it is difficult to model on the relatively large grid of the SDE. In order to release this heat a cloud must exist within certain limitations, there must be integrated vertical moisture convergence (M_t) in the atmospheric column, and the atmospheric column must have integrated difference between cloud and environmental temperatures. Convective latent heat release (CLHR) in the SDE is described by:

$$CLHR = \frac{g \ (1-b) \ L \ M_t \ [T_c(p)-T(p)] \ \frac{\theta}{T}}{(p_b-p_t) \ <T_c-T>} \tag{13}$$

It is important to remember that Kuo developed this cumulus parameterization scheme to represent tropical conditions. Using it over continental midlatitudes requires modifications (Lin and Smith, 1979; Edmon and Vincent, 1976). The modifications have been implemented as presented by Smith, Dare and Lin (1984), and Lin and Smith (1979).

Primary to the release of latent heat from convective activity, is the presence of deep convection. The SDE uses cloud parameters and definitions as presented by Edmon and Vincent (1976), and modified by Lin and Smith (1979). (For a flowchart depicting calculation of CLHR in the SEAM see Appendix B.) In the SDE a cloud base is defined to be at the level of free convection (LFC) for a grid point, while the top of the cloud is delimited by the equilibrium level (EL). If no EL is present then no cloud is considered to exist at a particular grid point. In order to be considered for calculation of CLHR, a cloud base must be between 1000 mb and 700 mb, with a thickness of at least 100 mb. In addition, convective instability must exist in order for CLHR to be present at any given level in the model. As observed in Appendix B and described above, the cumulus parameterization is quite complex and criteria for calculation of CLHR is restrictive.

A major portion of the algorithm is the calculation of integrated vertical moisture convergence (M_t) as presented by (14).

$$M_t = -\frac{1}{g} \int_{P_s}^{P_t} \left(\nabla_p \cdot \vec{V} q \right) dp + \rho_b C_D \left| \vec{V}_b \right| \left(q_s - q_b \right) \tag{14}$$

This parameterization, as used in the SDE, is based upon the Kuo (1974) scheme as

used by Edmon and Vincent (1976) and modified by Lin and Smith (1979). M_t represents the moisture available for cloud formation (Edmon and Vincent, 1976). Comprising (14) are a term representing the convergence of moisture in the column of air produced by large scale flow and a term for evaporation from the surface, respectively (Kuo, 1974). In the model, both u and v components of the wind used in the calculation of M_t are obtained using linear vertical interpolation from known values at levels in the model on either side of the LFC, previously defined to be the base of the cloud. In addition, wind and density at the cloud base are calculated for use in the second term of M_t. The drag coefficient (C_D) is the value found by Cressman (1960) to be representative of vegetated land areas (2.0×10^{-3}).

As previously discussed, the SEAM uses synoptic scale data on a 190.5 km grid. This causes difficulty in resolving smaller scale features such as the CLHR. The second term of (14) is an attempt to circumvent this problem. The addition of surface data to the model could allow for more accurate evaporation values from the surface. However, one of the limitations that would remain is that other entrainment is ignored.

Closely related to the integrated vertical moisture convergence is the b parameter, as seen in (13). This variable represents the fraction of M_t stored in the air to increase the specific humidity of the environment (Smith, Dare and Lin, 1984). Kuo (1974) suggests that b is much smaller than one in low level convergence zones. Keeping in mind that the scheme was originally designed for the tropics, Smith, Dare and Lin (1984) modified the use of the b parameter to a method similar to that used by Anthes (1977) and implemented in this study. This modified use of the b parameter is based upon the average RH from 1000 mb to 500 mb. The critical RH value of 0.80 is also used in calculation of CLHR for consistency throughout the model. If the average

RH is above this critical value then b is assigned the value of zero. If the average RH is below a minimum value (0.40) then b is assigned a value of 1. For average RH values between these two significant values b is assigned a value of 1 - RH. Referring to (13) one can see that all possible M_t is available when b is assigned the value of zero. Conversely when b is assigned a value of one, there can be no CLHR.

The final major portion of (13) is $<T_c - T>$. This term of the CLHR equation represents buoyancy, and is represented by:

$$<T_c - T> = \frac{1}{P_b - P_t} \int_{P_t}^{P_b} (T_c - T)\, dp \tag{15}$$

T_c represents the cloud temperature while T is the environmental temperature. T_c is calculated using FORTRAN routines from Doswell et al. (1982) which raises a parcel along the psuedoadiabat to the desired pressure level. Note that if $T \geq T_c$ then CLHR is not allowed (Haltiner and Williams, 1980). Therefore, if (14) is a negative value then CLHR is not allowed. The final computational procedure applied to the release of latent heating is the Laplacian operator.

Chapter 4: Case Studies and Analysis Model Output

This chapter describes the synoptic situation and SEAM output analyzed in the limited case comparison. Each case, explosive and normal cyclogenesis, are first presented as observed using surface and upper air data. Then the output of the SEAM is presented with relevant comparison to the observed data.

4.1 Synoptic Situation: Explosive Case

The explosive development case occurred from about 1200 UTC on 14 December 1987 to 0000 UTC on 16 December 1987. This storm developed in southeast Texas and tracked through Arkansas and Illinois before dissipating in Northern Michigan (Fig. 4-1a); with a period of rapid deepening from 15/00 UTC to 15/12 UTC (Fig. 4-1b). Significant amounts of snowfall were recorded with this storm (Fig. 4-2) with broad areas of 12 inch totals reported across Missouri and Illinois. Also, isolated areas with snowfalls of 16 inches were reported across the panhandle of Texas, Wisconsin and Michigan. A comparison of Fig. 4-1a, 4-1b and 4-2 reveals that the broad area of 12 inch snowfall in Missouri correspond with the location of strongest development from the St. Louis, Missouri area to southwest of Chicago, Illinois.

At 14/12 UTC, a deep upper level trough was over the Rockies with a strong jet core (65 m/s) at 300 mb exiting old Mexico (not shown) with an area of diffluence across the Great Plains. The 500 mb chart showed a closed low with 22×10^{-5} s^{-1} absolute vorticity in the base of the trough with a minor vorticity lobe downstream (not shown). The surface map for 14/12 UTC (Fig. 4-3) depicts a warm front along the Gulf coast with a broad area of precipitation from eastern New Mexico and Colorado
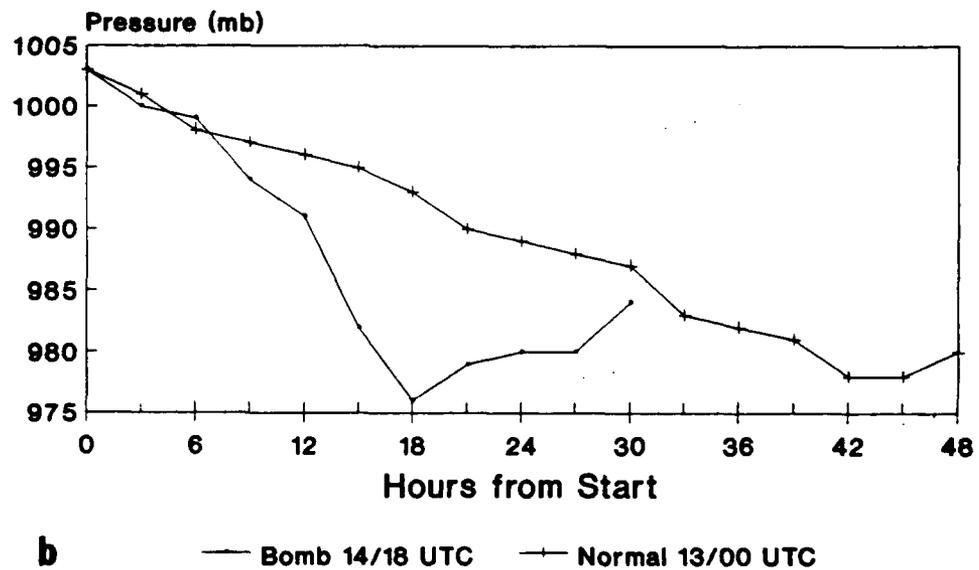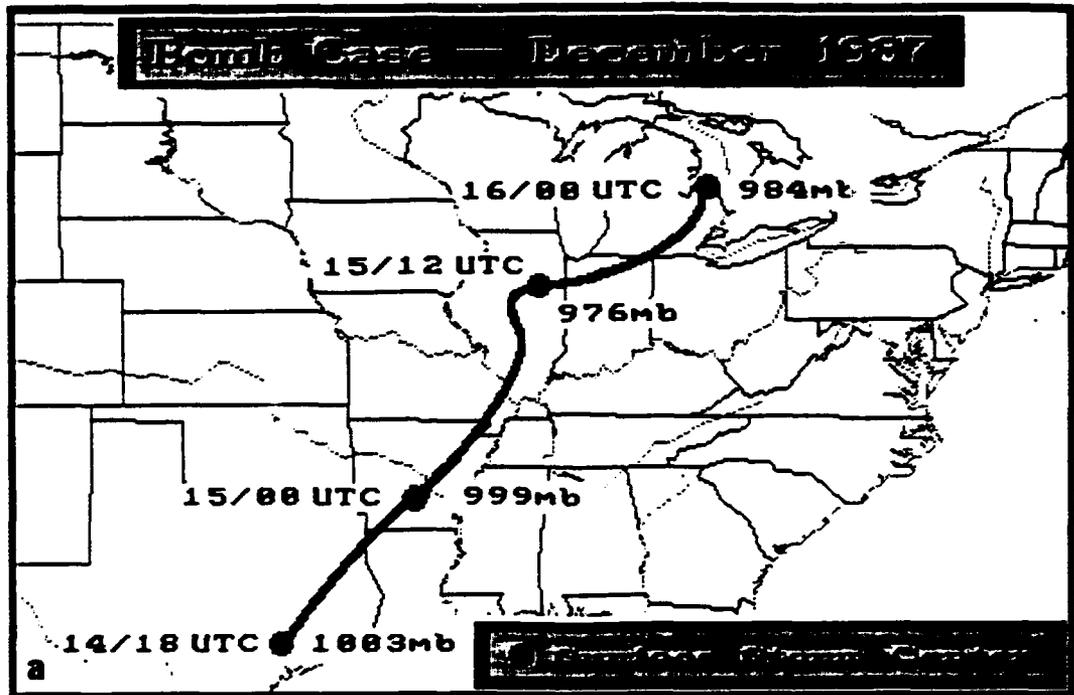
Figure 4-1. a) Explosive case storm track with 12 hour positions from 18 UTC 14 Dec 87 to 00 UTC 16 Dec 87. b) Central pressure trace for the bomb case (18 UTC 14 Dec 87 start) and the normal case (00 UTC 13 Feb 91 start).
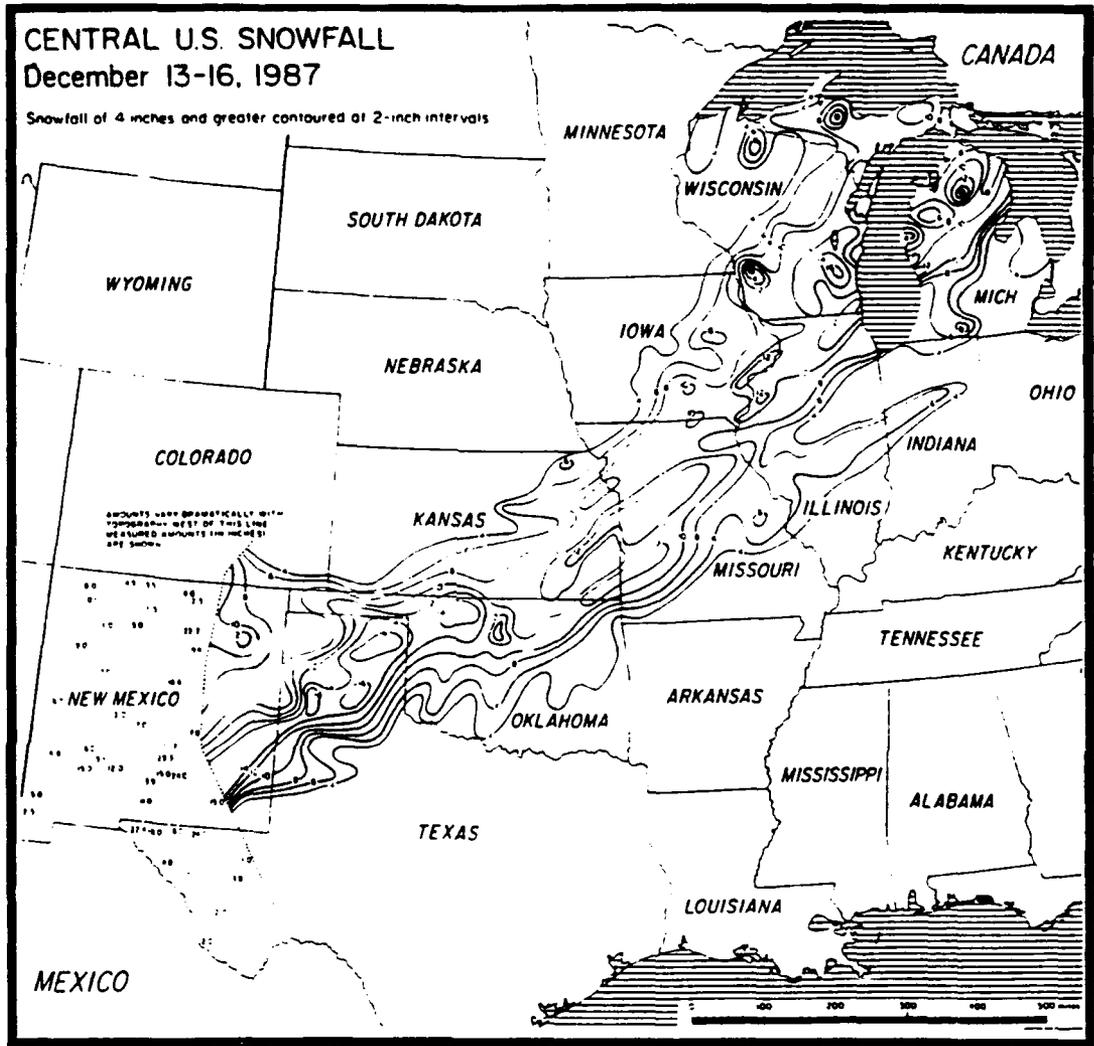
Figure 4-2. Snowfall distribution for 13-16 Dec 87 (Storm Data, 1987).
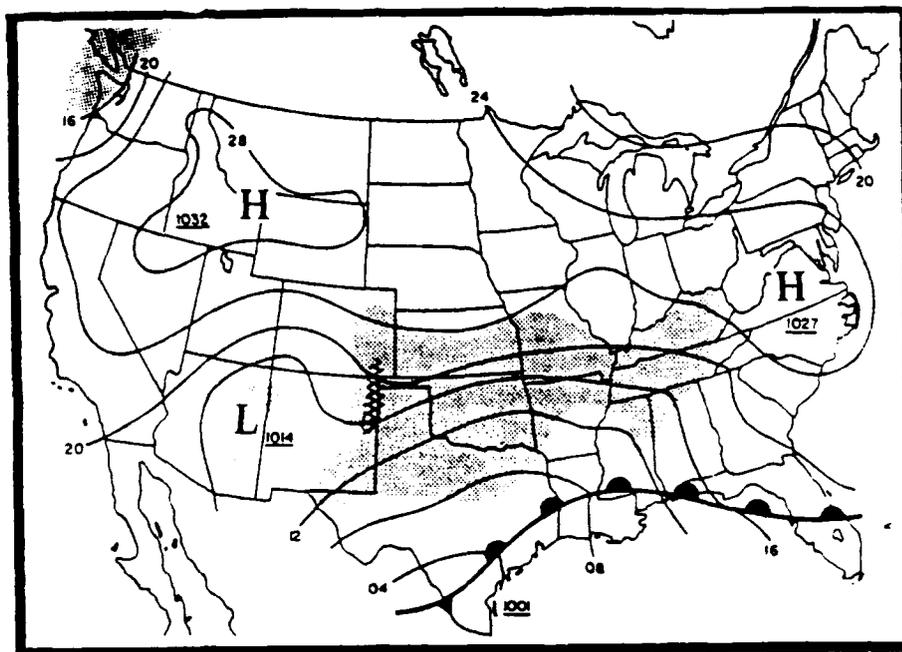
Figure 4-3. 12 UTC 14 Dec 87 Surface Analysis. Solid lines depict isobars (mb) with areas of precipitation shaded; areas of cross-hatching depict non-convective heavy precipitation (after Adams, 1989).

through Kentucky and Tennessee. The low at the surface associated with the upper level trough is evident in Arizona with a central pressure of 1014 mb. At this point in time, the low center is relatively weak and ill-defined.

By 14/18 UTC a closed low with central pressure of 1003 mb had developed in east Texas along the warm front in the Gulf coast region seen at 14/12 UTC (Fig. 4-3). The area of precipitation has moved to the north and generally increased. In addition, precipitation had begun along the Mississippi and Florida Gulf coast.

In the 15/00 UTC series of upper air charts the trough begins to take on a negative tilt. The 300 mb jet streak (not shown) increases to 75 m/s and begins to branch off through central Oklahoma and east through south Texas, providing significant diffluence. The 500 mb trough (not shown) maintains approximately the same strength as at 14/12 UTC but the area of positive vorticity has become more well defined. On the surface (Fig. 4-4a) the low is also more well defined with a central pressure of 999 mb. Precipitation areas are more organized also with stronger areas to the north and west of the low center. In addition the radar summary (Fig. 4-4b) shows a solid convective line echo from Arkansas to the Gulf of Mexico ahead of the cold front.

By 15/03 UTC the low pressure center, with a central pressure of 994 mb, moved to the boot heel area of Missouri with strong well-organized convection along the cold front extending to the Gulf. Significant areas of precipitation still extended from north through northwest of the low.

The 300 mb 15/12 UTC chart shows the amplitude of the trough increasing and continuing to lift northeastward with the 75 m/s jet streak extending from Arkansas
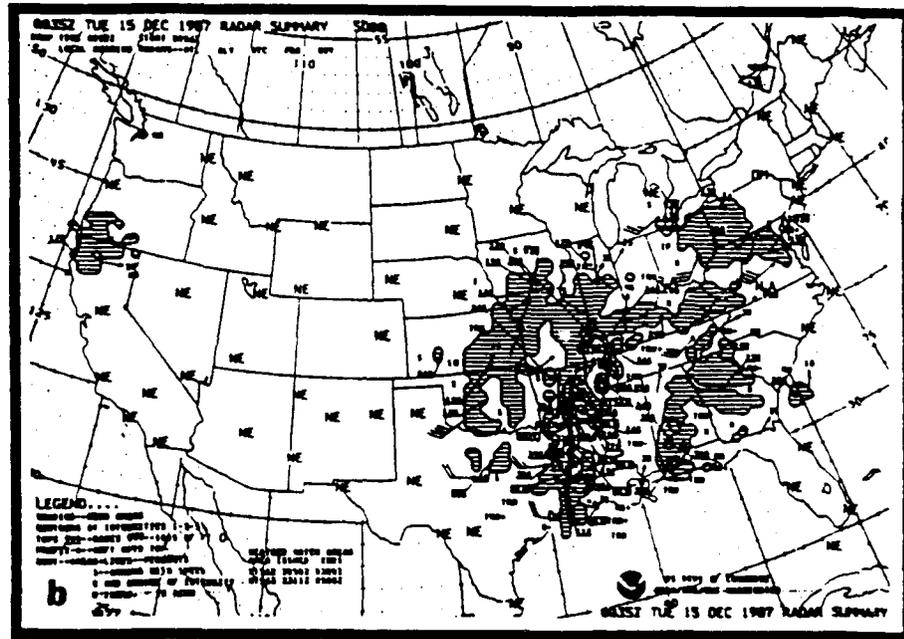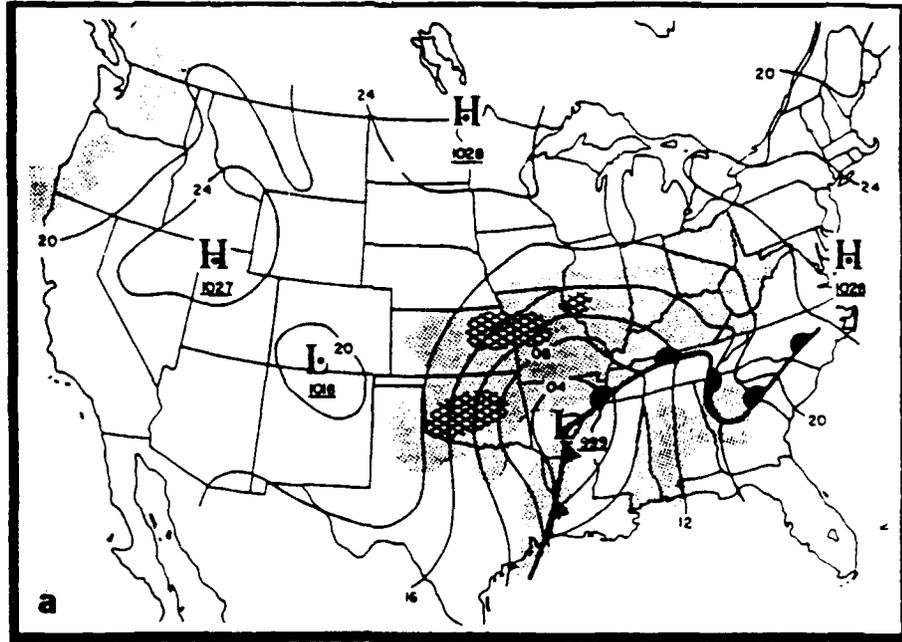
Figure 4-4. **a)** 00 UTC 15 Dec 87 Surface Analysis. Solid lines depict isobars (mb) with areas of precipitation shaded; areas of cross-hatching depict non-convective heavy precipitation. **b)** 0035 UTC 15 Dec 87 NWS Radar Summary (after Adams, 1989).

into central Indiana around the base of the trough (not shown). At 500 mb the strong vorticity maximum is sustained and centered near St. Louis, Missouri at 15/12 UTC (Fig. 4-5a). At the surface (Fig. 4-5b) the system was occluded and continued to deepen to a central pressure of 976 mb, the lowest for the lifetime of the storm. This represents a 23 mb drop in central pressure over the last 12 hours.

Upper level support at 300 mb (not shown) for the storm had dissipated by 16/00 UTC. The storm was vertically stacked as well with a secondary cyclogenesis center developing on the remaining cold front on the Atlantic coast (Fig. 4-6). The central pressure of the storm as it moved over Michigan climbed to 984 mb.

4.2 SEAM Output: Explosive Case

The SEAM was run for each 12 hour period during the storm. Values for each term are presented in a figure with the Sutcliffe value being the total of each term as presented by (1). Figures for all terms including the Sutcliffe value are presented for all time periods regardless of text reference for study and review at the readers discretion.

At 14/12 UTC Sutcliffe term values are positive in south central Texas (Fig. 4-7a) and central Kansas. This former area corresponds well with the site of initial development of the storm at 14/18 UTC (Fig. 4-1). This positive area of 60 to 120 units is located just north of the frontal zone along the Texas Gulf coast. Note that the area of initial development is near the grid edge so errors associated with linear extrapolation must be taken into account when an interpretation is made.

Figure 4-5. a) 12 UTC 15 Dec 87 500mb Analysis. Solid lines -- same as the 300mb analysis; dashed lines depict absolute vorticity ($10^{-5}s^{-1}$) with "X" denoting vorticity maxima and "N" vorticity minima (after Adams, 1989). **b)** 12 UTC 15 Dec 87 Surface Analysis. Solid lines depict isobars (mb) with areas of precipitation shaded; areas of cross-hatching depict non-convective heavy precipitation (after Adams, 1989).

Figure 4-6. 00 UTC 16 Dec 87 Surface Analysis. Solid lines depict isobars (mb) with areas of precipitation shaded; areas of cross-hatching depict non-convective heavy precipitation (after Adams, 1989).
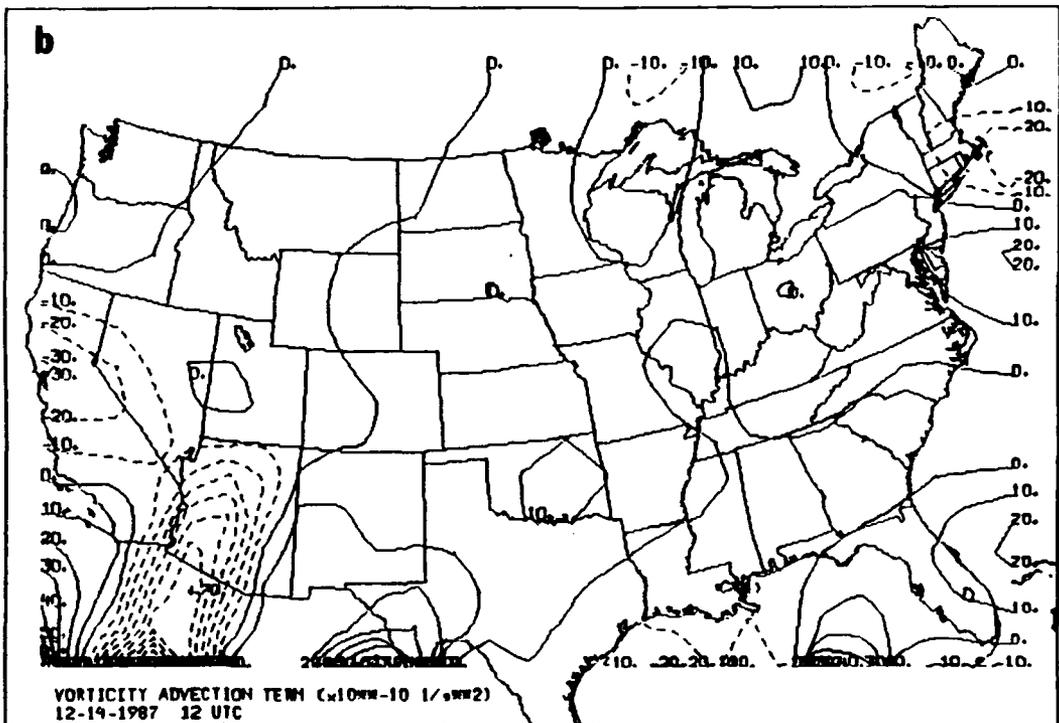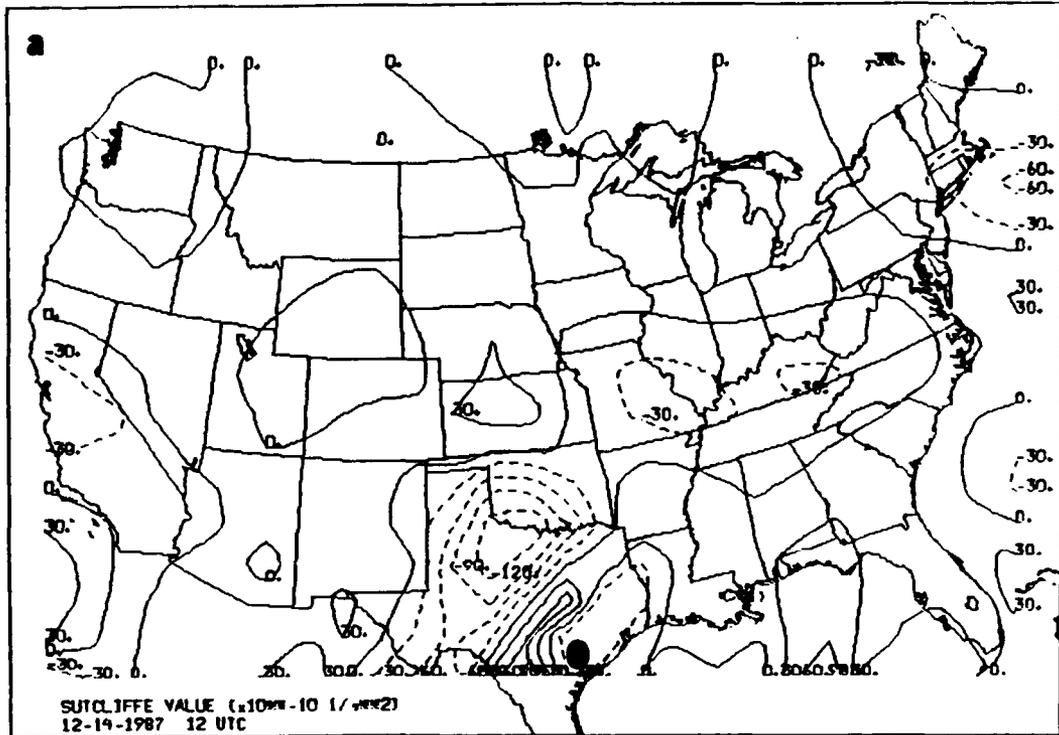
Figure 4-7. a) Sutcliffe Equation Analysis Model total values for 12 UTC 14 Dec 87 (10^{-10} s^{-2}). Dot is surface storm center. Solid lines are positive values and dashed lines are negative values. **b)** Vorticity Advection Term values for 12 UTC 14 Dec 87 (10^{-10} s^{-2}). Solid lines are positive values and dashed lines are negative values.

In this initial time period the thickness, stability and heating terms (Fig. 4-7c,d,e respectively) tend to dominate. The thickness and stability terms have relatively large negative values from Texas through Kentucky, while the heating term shows positive values in this area. Note the positive area in Kansas and Nebraska on the Sutcliffe chart (Fig. 4-7a). This is a result of the strong positive raw stability term values in this area (Fig. 4-7f). Raw stability values consist of S_a which are S_m and S_d combined as described in section 3.3.3. Note that despite the fact that the atmosphere displays static instability (10c) in the Texas - Oklahoma area, the Sutcliffe value is negative, indicating no cyclonic development. This is due to the braking effect of the stability term as previously discussed. The apparent difference between Kansas and south Texas on the Sutcliffe chart is the synergism between the terms.

Higher Sutcliffe values in Texas appear at the 15/00 UTC time period (Fig. 4-8a). Once again, edge effects magnify the values along the southern border of the chart. In contrast to the previous period, all terms are of the same order of magnitude at 15/00 UTC. The heating term (Fig. 4-8e) has values that are slightly smaller than the stability term (Fig. 4-8d) but the configuration of the raw latent heating values (Fig. 4-8f) match the precipitation pattern (Fig. 4-4d) well. Raw latent heating values are the sum of CLHR and SLHR. Figure 4-8f shows that CLHR values are quite small compared to SLHR values, although the CLHR values do coincide with the strong convective activity in Louisiana and Mississippi. Note how the negative stability values successfully counteract the vorticity and thickness terms (Figs. 4-8b,c) from eastern Oklahoma through Missouri. This configuration allows the heating term (Fig. 4-8e) to have significant influence despite the slightly smaller values, particularly in the southeastern Missouri and northern Arkansas area.

THICKNESS ADVECTION TERM (x10**-10 1/s**2)
12-14-1987 12 UTC

STABILITY TERM (x10**-10 1/s**2)
12-14-1987 12 UTC
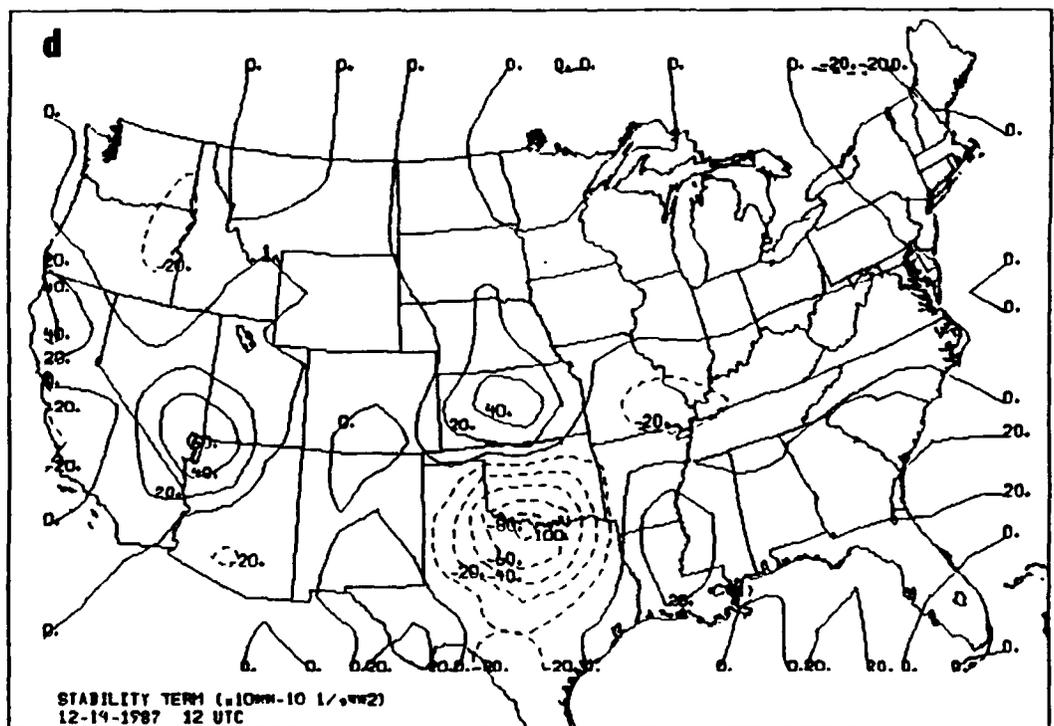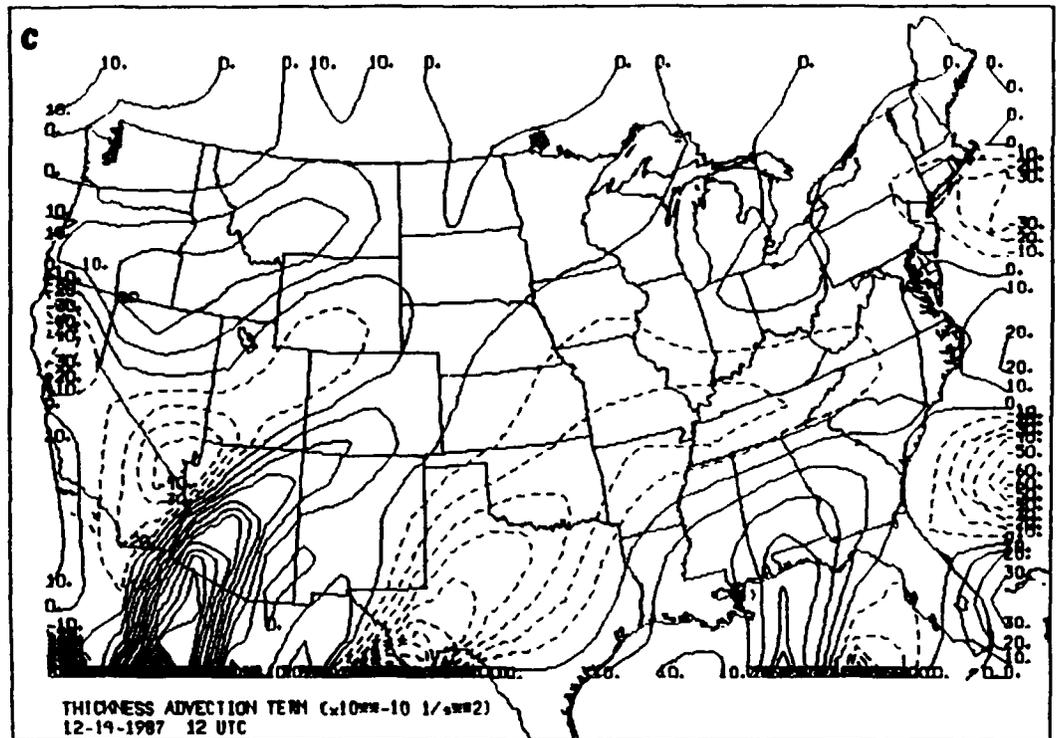
Figure 4-7. c) Thickness Advection Term values for 12 UTC 14 Dec 87 (10^{-10} s^{-2}). Solid lines are positive values and dashed lines are negative values. **d)** Stability Term values for 12 UTC 14 Dec 87 (10^{-10} s^{-2}). Solid lines are positive values and dashed lines are negative values.
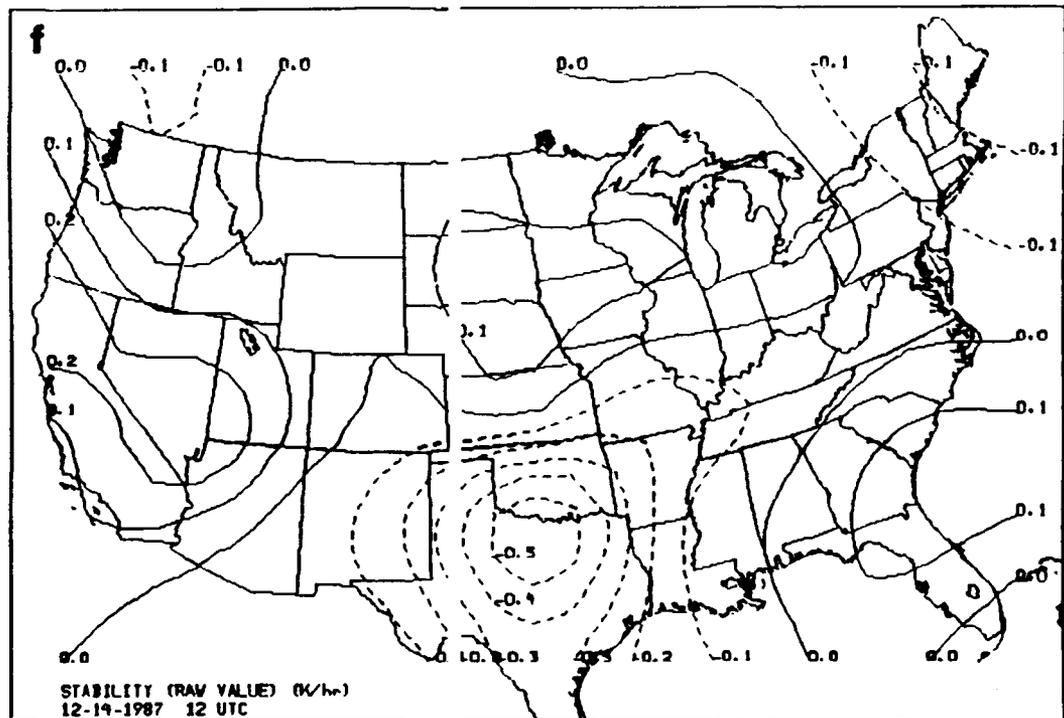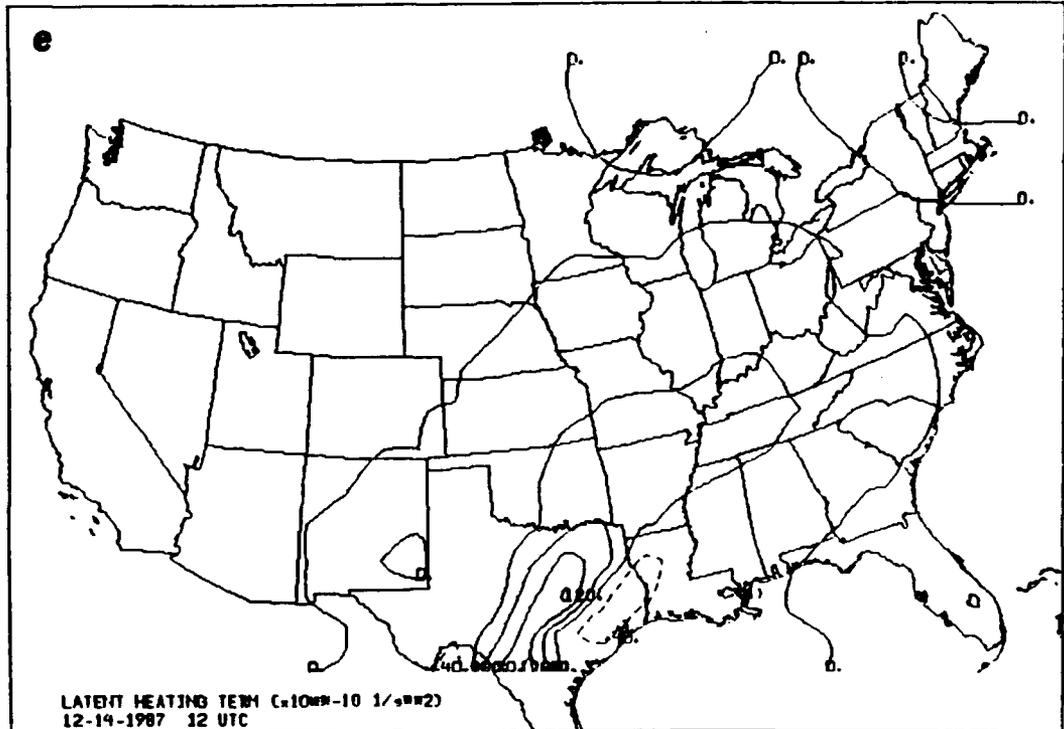
Figure 4-7. e) Latent Heating Term values for 12 UTC 14 Dec 87 (10^{-10} s^{-2}). Solid lines are positive values and dashed lines are negative values. **f)** Raw stability values for 12 UTC 14 Dec 87 (Khr^{-1}). Solid lines are positive values and dashed lines are negative values.
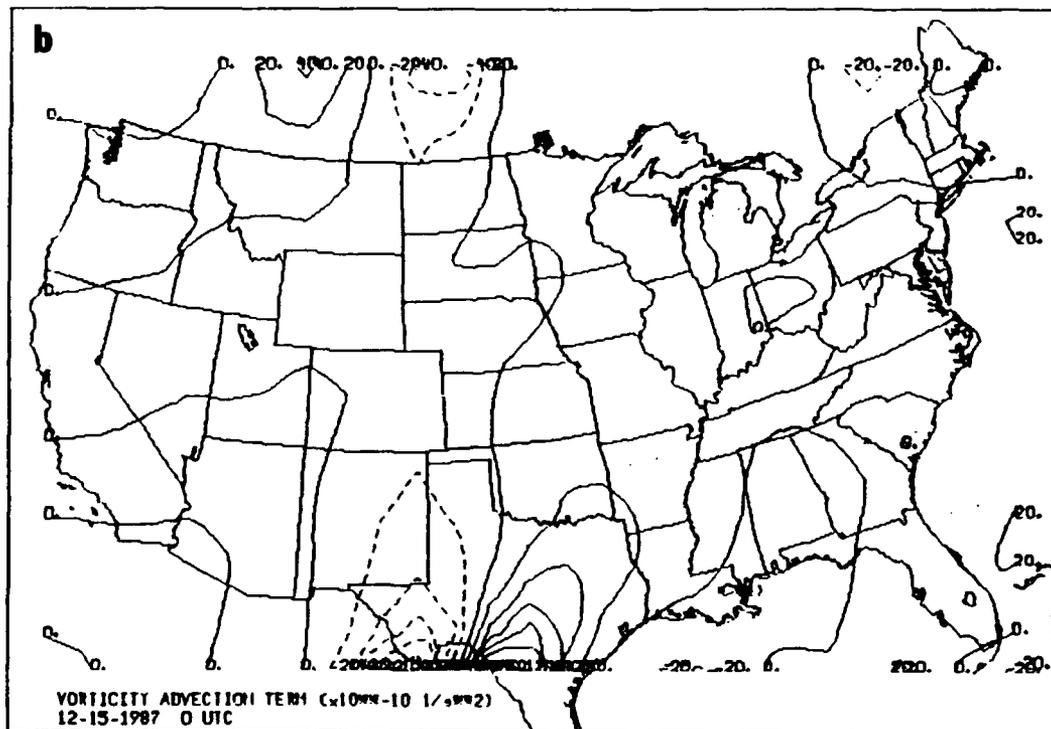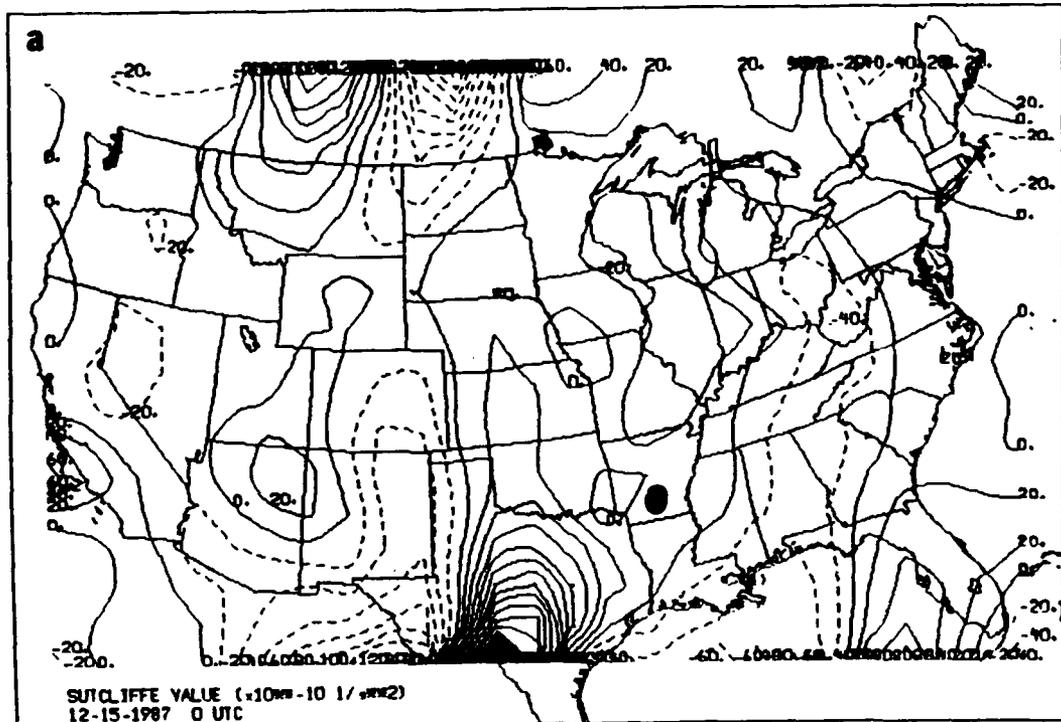
Figure 4-8. a) Sutcliffe Equation Analysis Model total values for 00 UTC 15 Dec 87 $(10^{-10} \text{ s}^{-2})$. Dot is surface storm center. Solid lines are positive values and dashed lines are negative values. b) Vorticity Advection Term values for 00 UTC 15 Dec 87 $(10^{-10} \text{ s}^{-2})$. Solid lines are positive values and dashed lines are negative values.
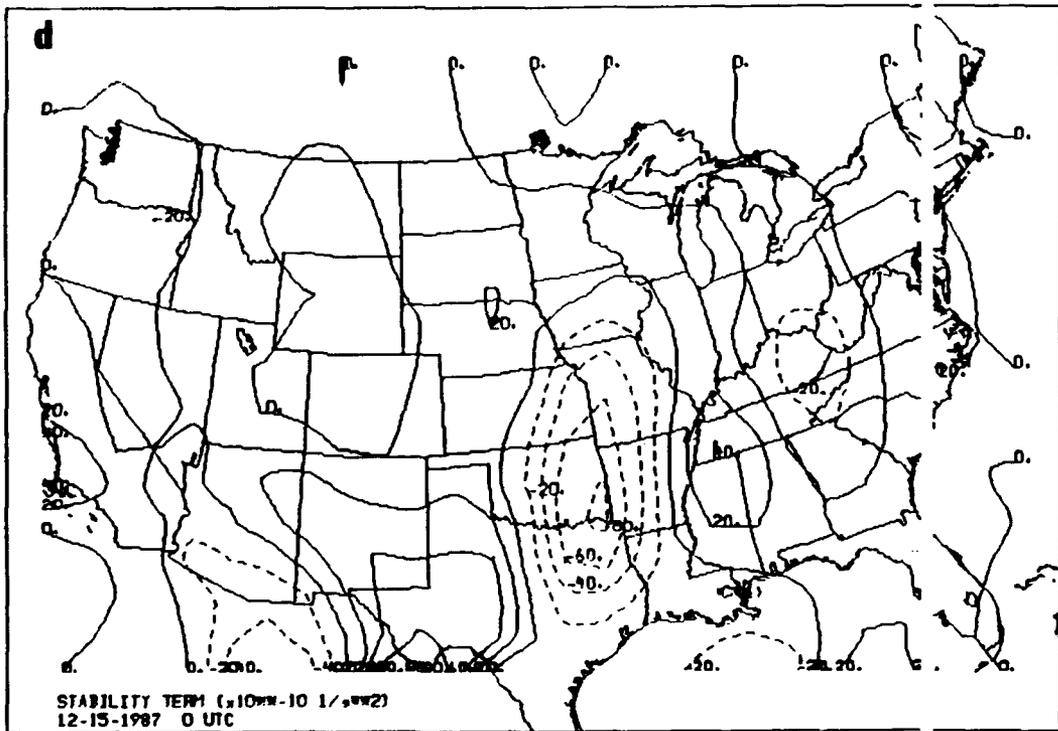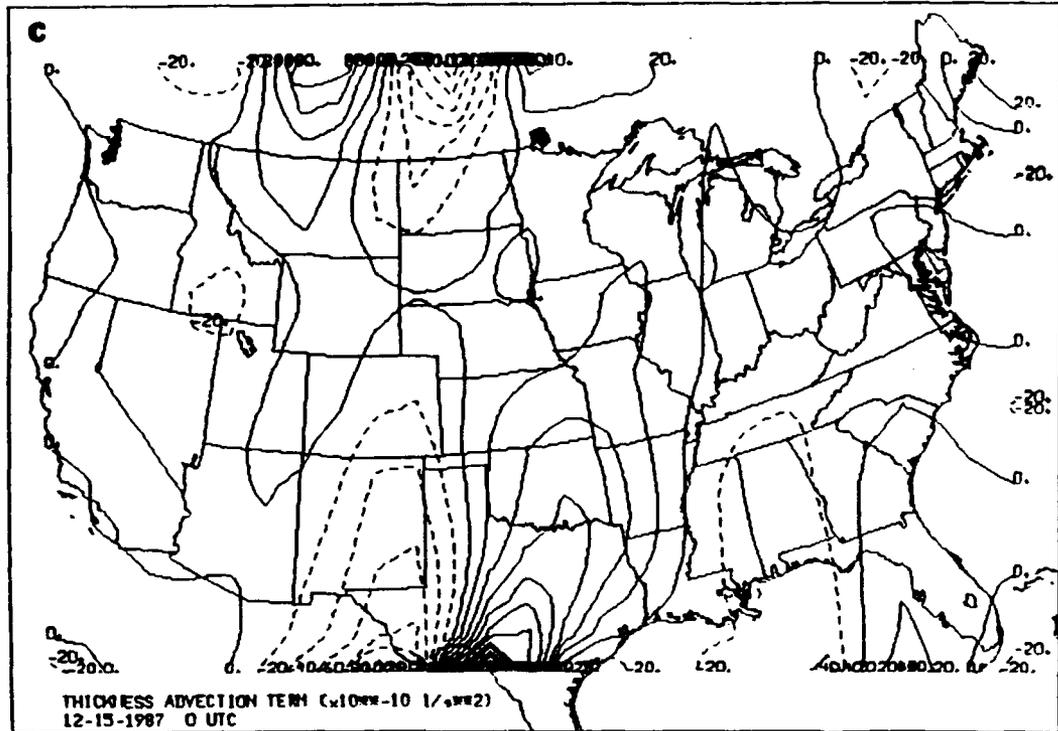
Figure 4-8. **c)** Thickness Advection Term values for 00 UTC 15 Dec 87 (10^{-10} s^{-2}). Solid lines are positive values and dashed lines are negative values. **d)** Stability Term values for 00 UTC 15 Dec 87 (10^{-10} s^{-2}). Solid lines are positive values and dashed lines are negative values.
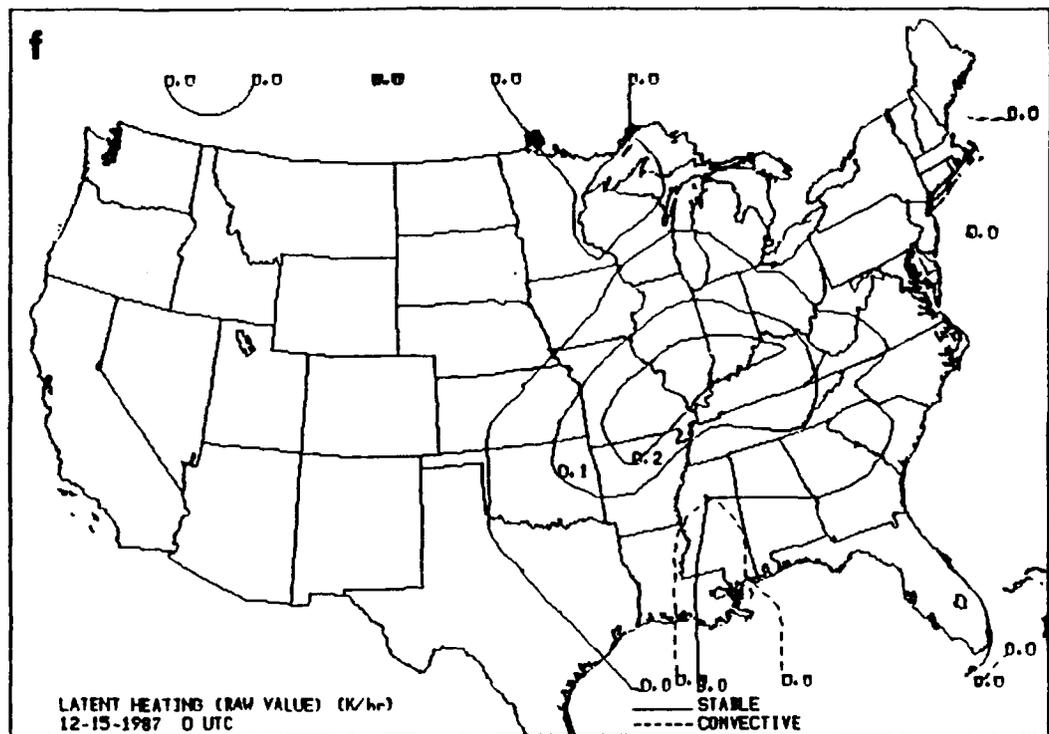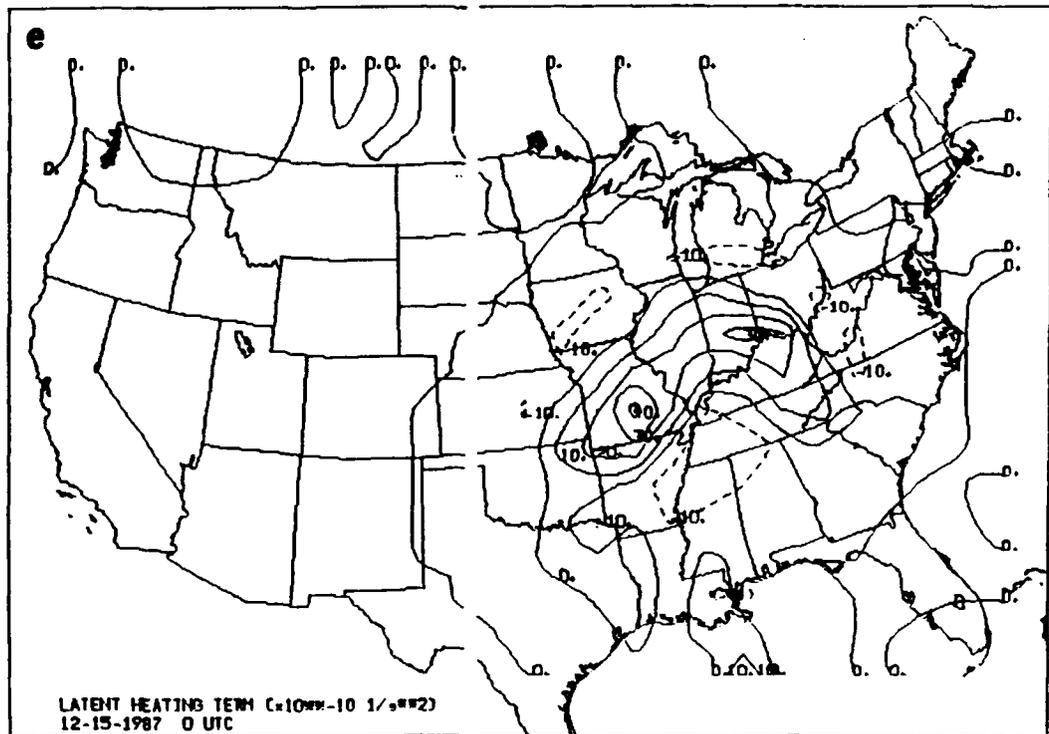
Figure 4-8. e) Latent Heating Term values for 00 UTC 15 Dec 87 (10^{-10} s^{-2}). Solid lines are positive values and dashed lines are negative values. **f)** Raw latent heating values for 00 UTC 15 Dec 87 (Khr^{-1}). Solid lines are SLHR and dashed lines are CLHR.

The surface storm center at 00 UTC (Fig. 4-1a) is in central Arkansas. The heating term shows values well wrapped around the surface pressure center.

It is of interest to note that in their study of explosive oceanic cyclogenesis along the east coast of the United States, Kocin and Uccellini (1990) found strong precipitation to the north and west of the storm center coincident with rapid surface development. This heating configuration in combination with values from the other terms creates a Sutcliffe maximum region from southern Missouri through Wisconsin (Fig. 4-8a). In comparison to Fig. 4-1a, the position of the low center, as it moved over Arkansas and southern Illinois for next twelve hours (15/00 to 15/12 UTC), corresponds directly to this ridge of Sutcliffe values (Fig. 4-8a).

The 15/12 UTC time period marks the turning point for the storm. The surface central pressure began to increase (Fig. 4-1b) and the Sutcliffe (Fig. 4-9a) values are now negative over the surface storm center for the first time in the life of this storm. Also take note of the fact that positive Sutcliffe values ahead of the storm are spatially limited with only a small maximum center over Lake Erie.

The vorticity and thickness terms (Fig. 4-9b,c) show more organized couplet patterns than in previous time periods. Stability and latent heating terms showed organized patterns in past time periods as now, but the vorticity and thickness terms begin to dominate the Sutcliffe output values. In comparison to Fig. 4-5c, the raw latent heating value (Fig. 4-9f) appears to be representative of the pattern of precipitation. Therefore, the heating term (Fig. 4-9e) is similarly representative.

Once again the values upwind of the storm do not appear to be relevant to actual development of the surface cyclone. This is demonstrated by the large positive
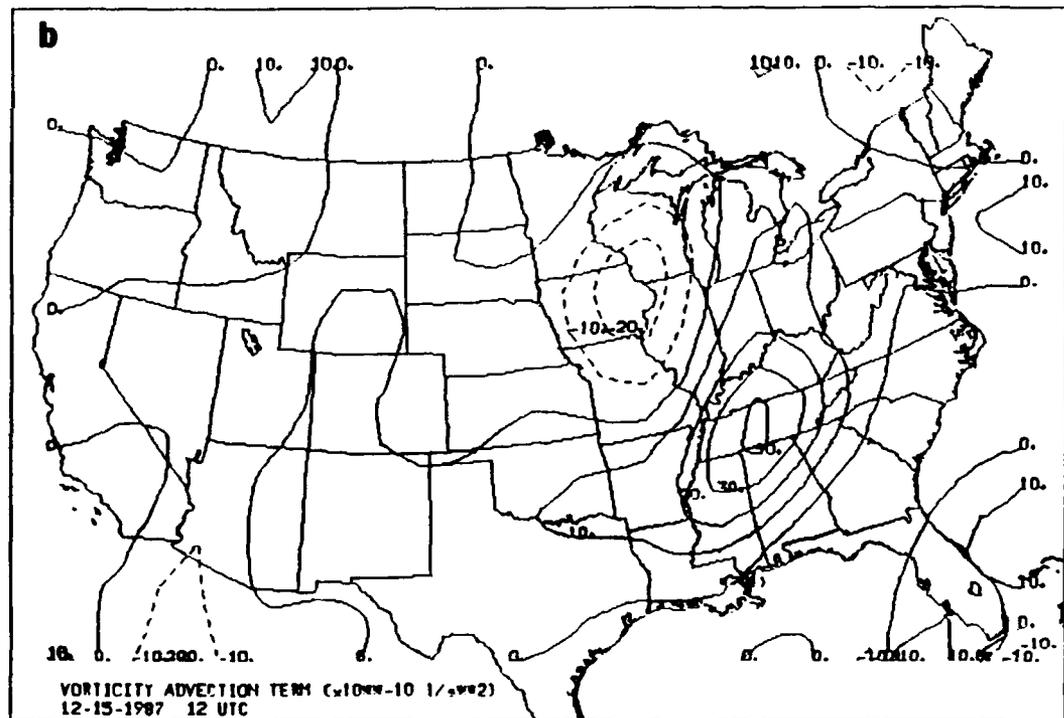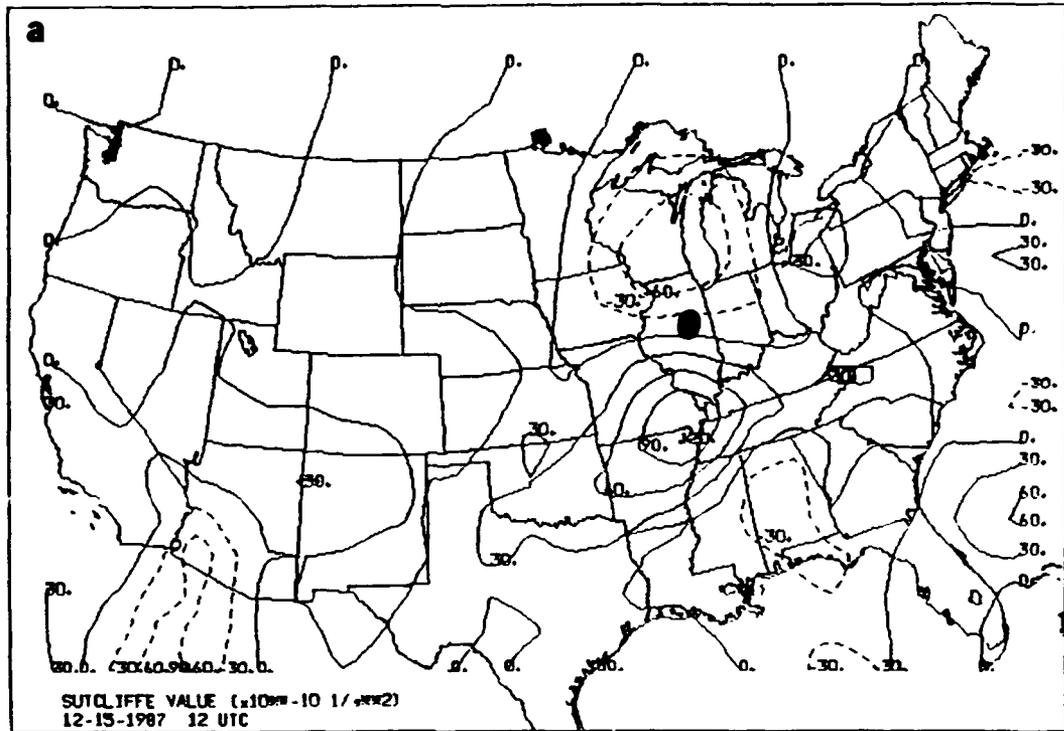
Figure 4-9. **a)** Sutcliffe Equation Analysis Model total values for 12 UTC 15 Dec 87 $(10^{-10} \ s^{-2})$. Dot is surface storm center. Solid lines are positive values and dashed lines are negative values. **b)** Vorticity Advection Term values for 12 UTC 15 Dec 87 $(10^{-10} \ s^{-2})$. Solid lines are positive values and dashed lines are negative values.

c) THICKNESS ADVECTION TERM (x10**-10 1/s**2)
12-15-1987 12 UTC

d) STABILITY TERM (x10**-10 1/s**2)
12-15-1987 12 UTC
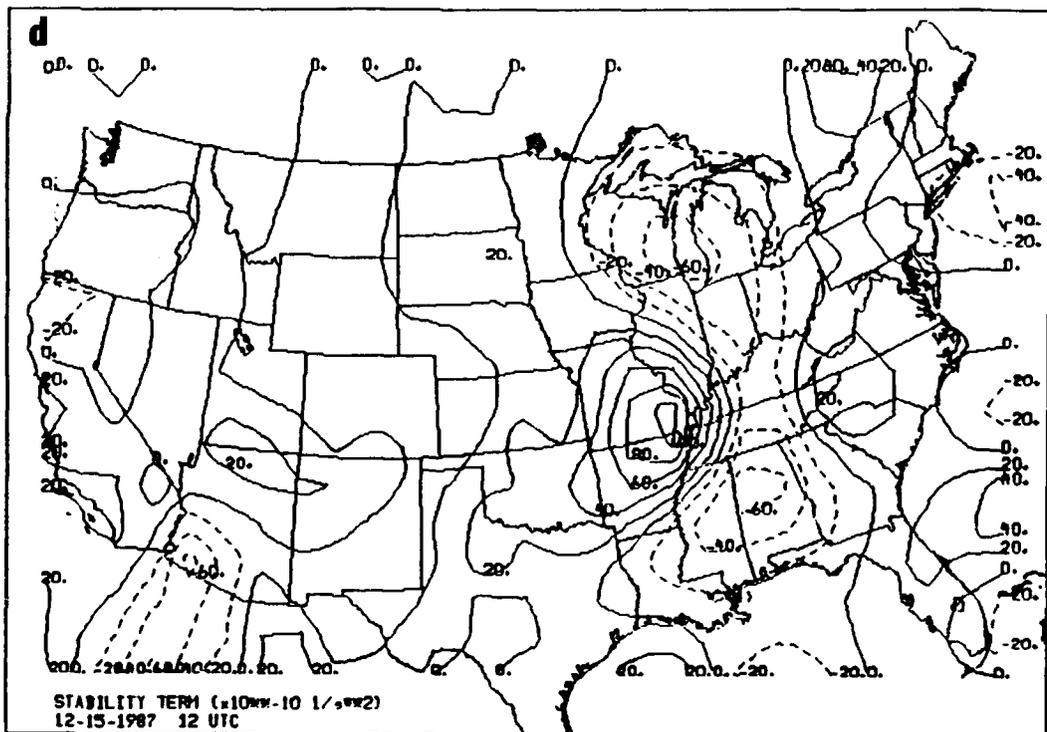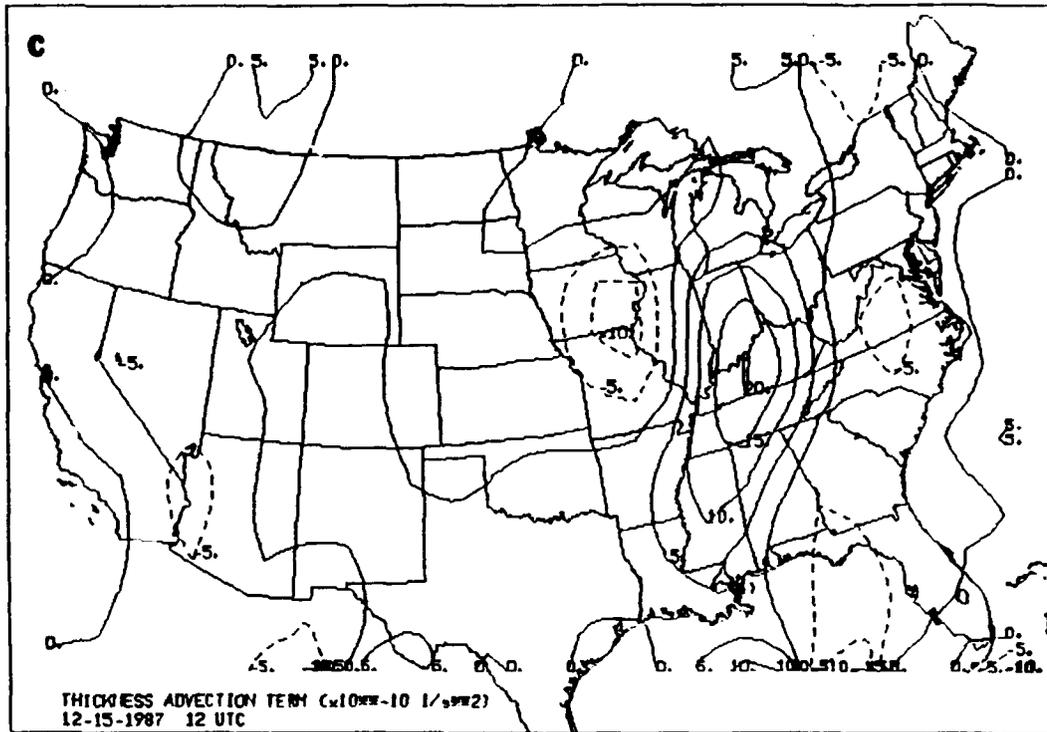
Figure 4-9. **c)** Thickness Advection Term values for 12 UTC 15 Dec 87 (10^{-10} s^{-2}). Solid lines are positive values and dashed lines are negative values. **d)** Stability Term values for 12 UTC 15 Dec 87 (10^{-10} s^{-2}). Solid lines are positive values and dashed lines are negative values.
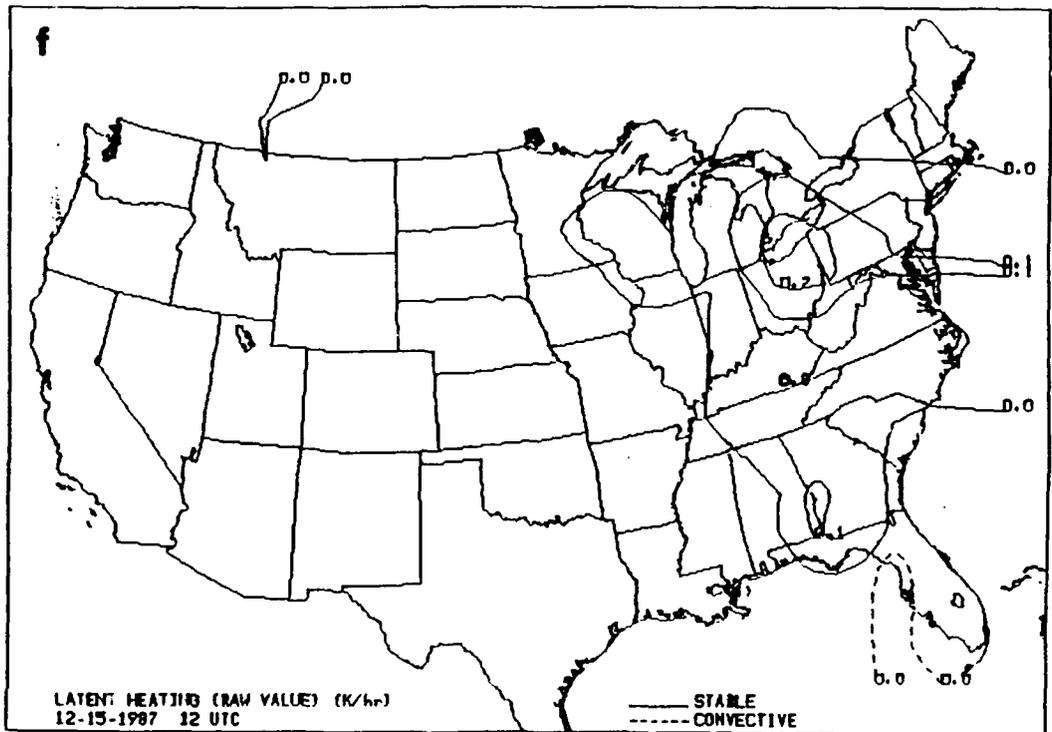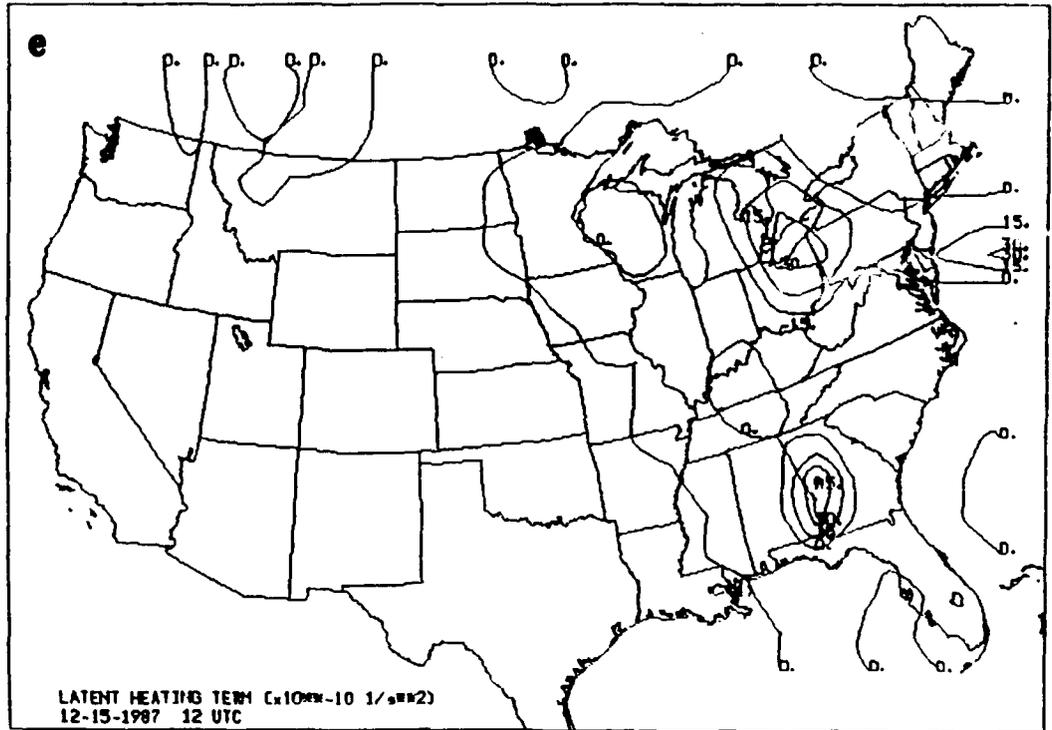
Figure 4-9. e) Latent Heating Term values for 12 UTC 15 Dec 87 (10^{-10} s^{-2}). Solid lines are positive values and dashed lines are negative values. f) Raw latent heating values for 12 UTC 15 Dec 87 (Khr^{-1}). Solid lines are SLHR and dashed lines are CLHR.

values in the boot heel region of Missouri despite the fact that this region is behind the front in an area of non-development. It is becoming quite obvious that proper interpretation of these product require a significant knowledge of the synoptic pattern and surface conditions. It appears as though Sutcliffe values at and downstream of the surface storm center are what need to be evaluated to estimate current and future development.

By 16/00 UTC the occluded low had moved over east Michigan and continued to fill (Fig. 4-1b). Sutcliffe (Fig. 4-10) values are featureless with the exception of the high values over Kentucky which is primarily a result of the stability term (not shown) as at 15/12 UTC. Other terms show the weak patterns.

4.3 Synoptic Situation: Normal Case

The normal case began at about 00 UTC on 13 Feb 91 and deepened slowly over the next 40 hours, reaching a minimum central pressure of 978 mb (Fig. 4-1b). The storm developed in the panhandle region of Texas and Oklahoma, travelled steadily to the Kansas City area and eastward across Missouri toward Lake Ontario (Fig. 4-11). A closed surface low formed around 13/00 UTC but significant weather was not seen until about 06 UTC when precipitation began to intensify and increase in areal coverage.

The 13/12 UTC surface chart (Fig. 4-12a) shows the low on the Kansas - Missouri border with a central pressure of 996 mb. By this time there is a relatively wide area of precipitation with rain and rainshowers extending from northeast Texas through southern Indiana. No thunderstorms were reported on the 1335 UTC radar
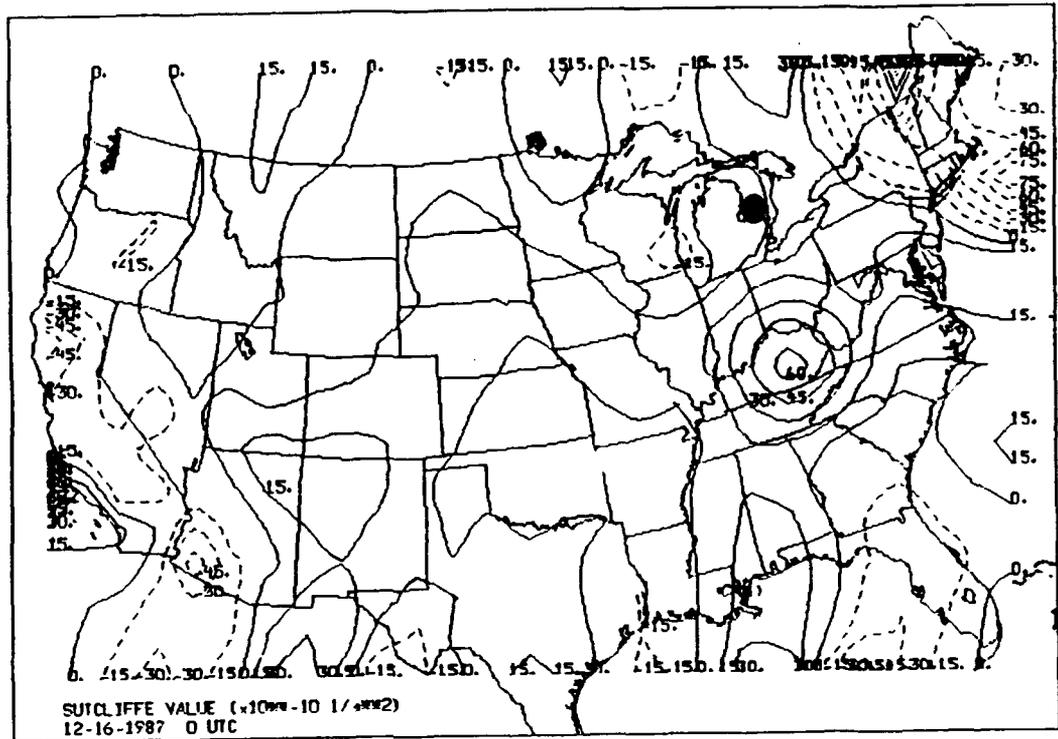
Figure 4-10. Sutcliffe Equation Analysis Model total values for 00 UTC 16 Dec 87 (10^{-10} s^{-2}). Dot is surface storm center. Solid lines are positive values and dashed lines are negative values.
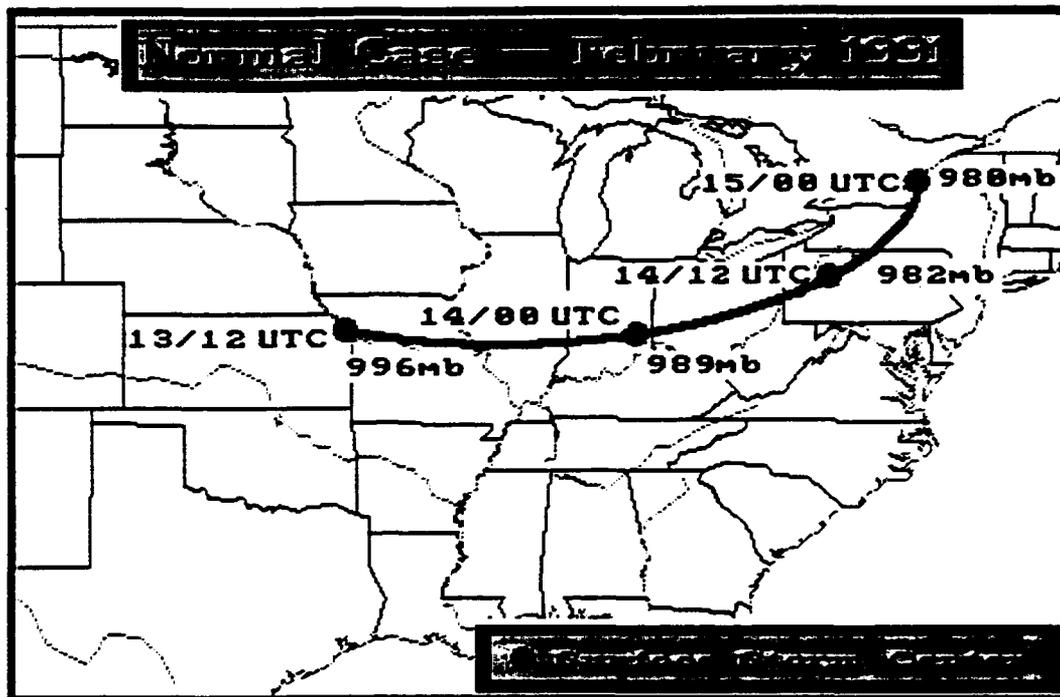
Figure 4-11. Normal case storm track with 12 hour positions from 12 UTC 13 Feb 91 to 00 UTC 15 Feb 91.
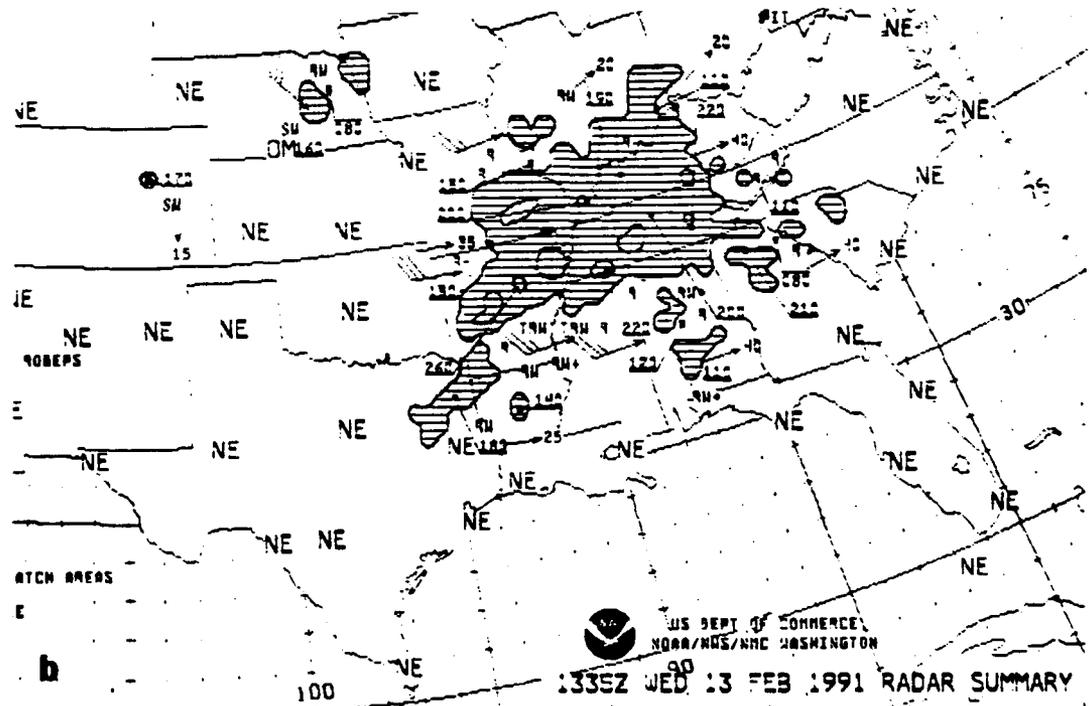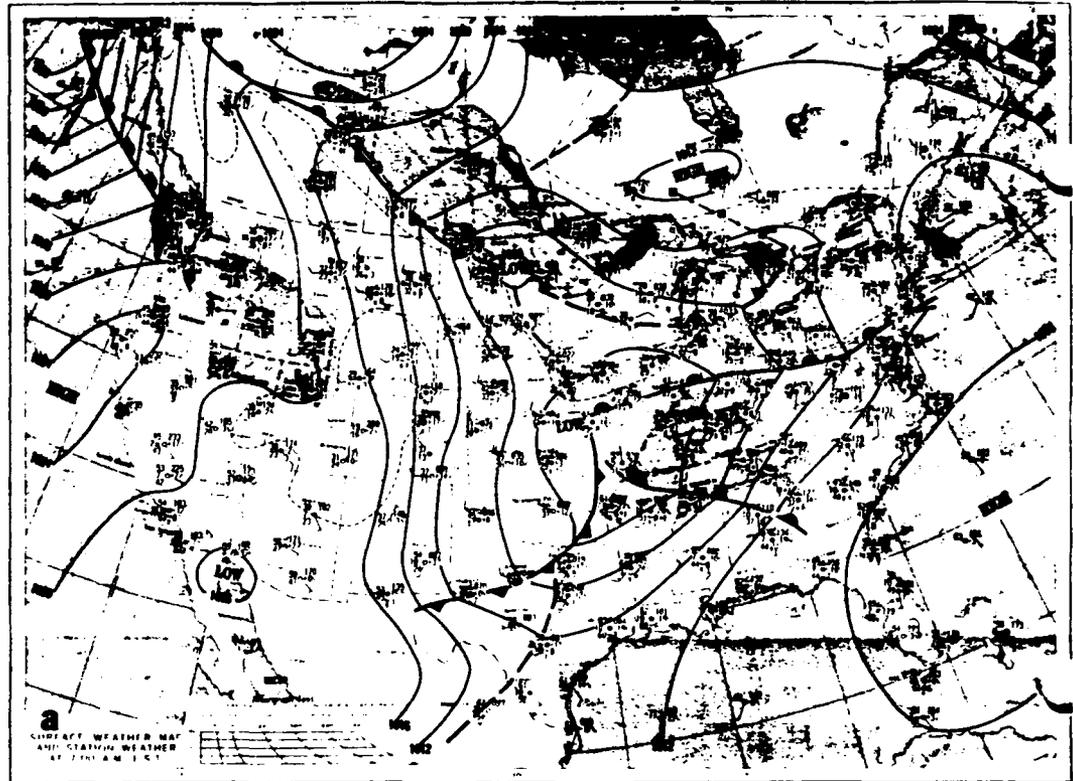
Figure 4-12. a) Surface chart for 12 UTC 13 Feb 91. Solid lines depict sea level pressure (mb) and precipitation areas are shaded (NOAA, 1991). b) 1335 UTC 13 Feb 91 NWS National Radar Summary.
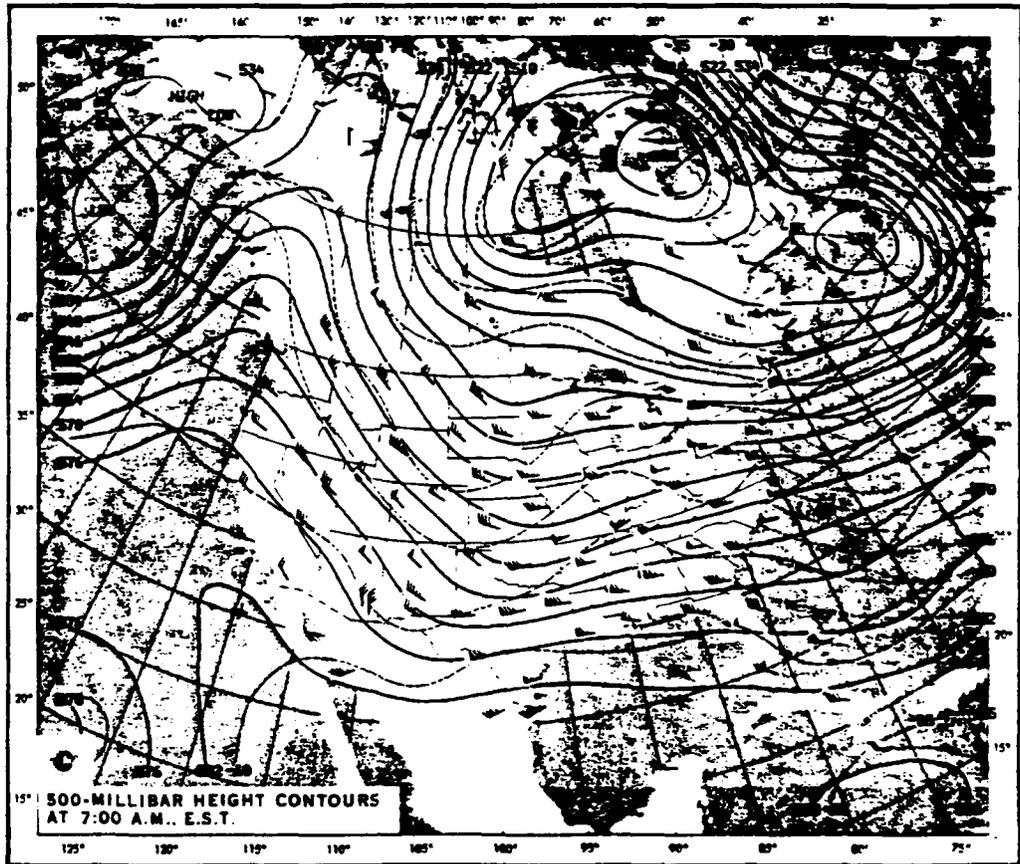
Figure 4-12c. 12 UTC 13 Feb 91 500mb Analysis. Solid lines depict geopotential height (decameters); dashed lines depict isotherms (C) (NOAA, 1991).

summary (Fig. 4-12b). At 300 mb (not shown), a 50 m/s jet streak was moving from the northwest United States into the area of the storm, joining with the subtropical jet. There is some diffluence in the Arkansas - Missouri area and eastward at this level as well. A shortwave trough is visible at 500 mb (Fig. 4-12c).

The storm continued to develop slowly and by 14/00 UTC it reached 989 mb at the surface (not shown). The base of the 500 mb trough had moved into Iowa and south to the Louisiana Gulf Coast (Fig. 4-13a). However, the 300 mb jet maximum was past the base of the trough by this time (not shown). Precipitation covered nearly the entire Ohio and Tennessee Valleys. In addition, strong thunderstorms were in progress in western Tennessee (Fig. 4-13b). Some thunderstorms were also occurring on the Mississippi Gulf coast but were too far from the storm center to contribute to development. The thunderstorms continued moving east with the system but remained isolated over land. By 14/08 UTC thunderstorms over the Gulf of Mexico became more organized, forming a solid line echo on the radar chart.

At 14/12 UTC strong 300 mb northwesterly flow from Canada intensified the trough/ridge pattern which increased in amplitude. The shortwave trough at 500 mb (Fig. 4-14a) continued to move through the Mississippi valley with the broad base of the trough through Illinois, Tennessee and Georgia. The surface analysis (Fig. 4-14b) shows the storm beginning to occlude in Pennsylvania at this time, but it continued to deepen slowly with a central pressure of 982 mb. Much of the precipitation had ceased by this time (Fig. 4-14c) with snow and freezing rain continuing in the northeast and the only remaining thunderstorms in Florida.

Figure 4-13. a) 00 UTC 14 Feb 91 500mb Analysis. Solid lines depict geopotential height (decameters); dashed lines depict isotherms (C). b) 0035 UTC 14 Feb 91 NWS National Radar Summary.
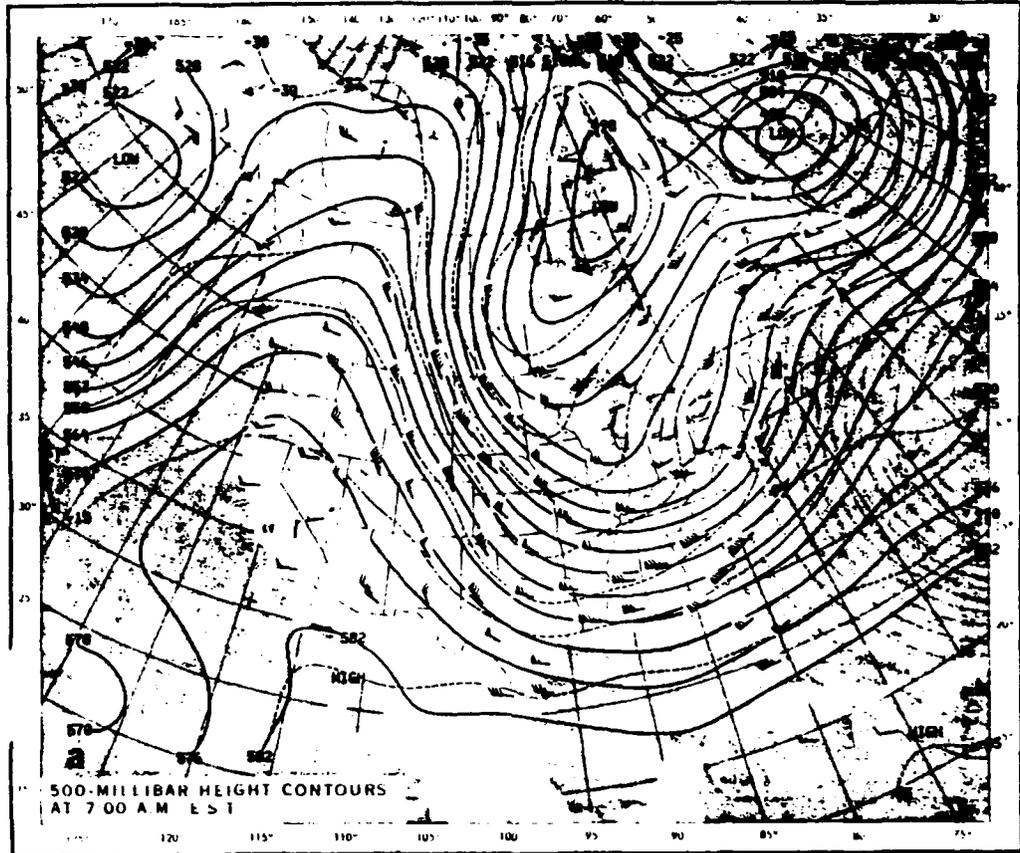
Figure 4-14a. 12 UTC 14 Feb 91 500mb Analysis. Solid lines depict geopotential height (decameters); dashed lines depict isotherms (C) (NOAA, 1991).
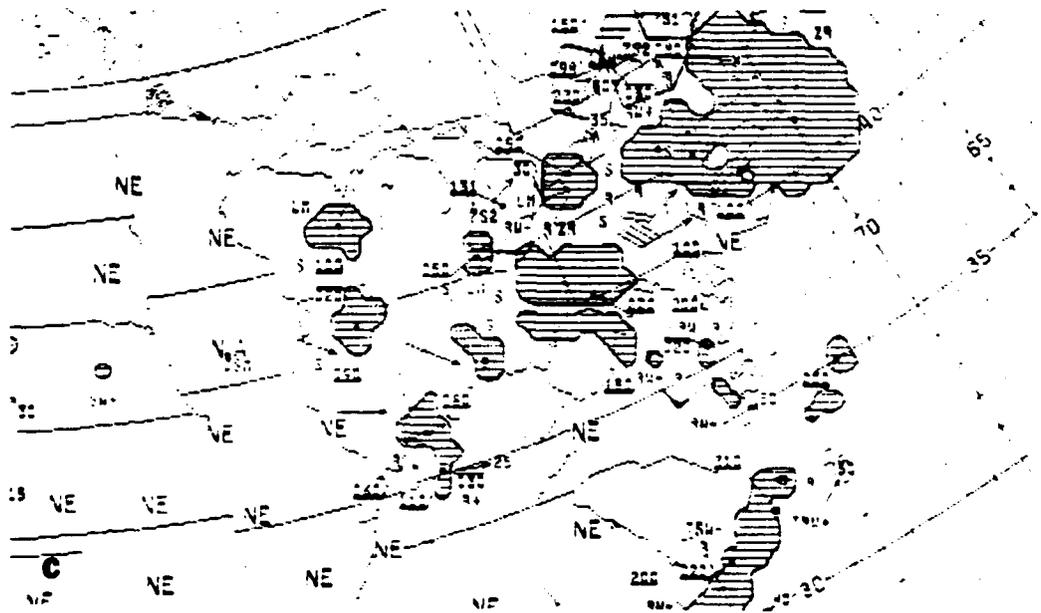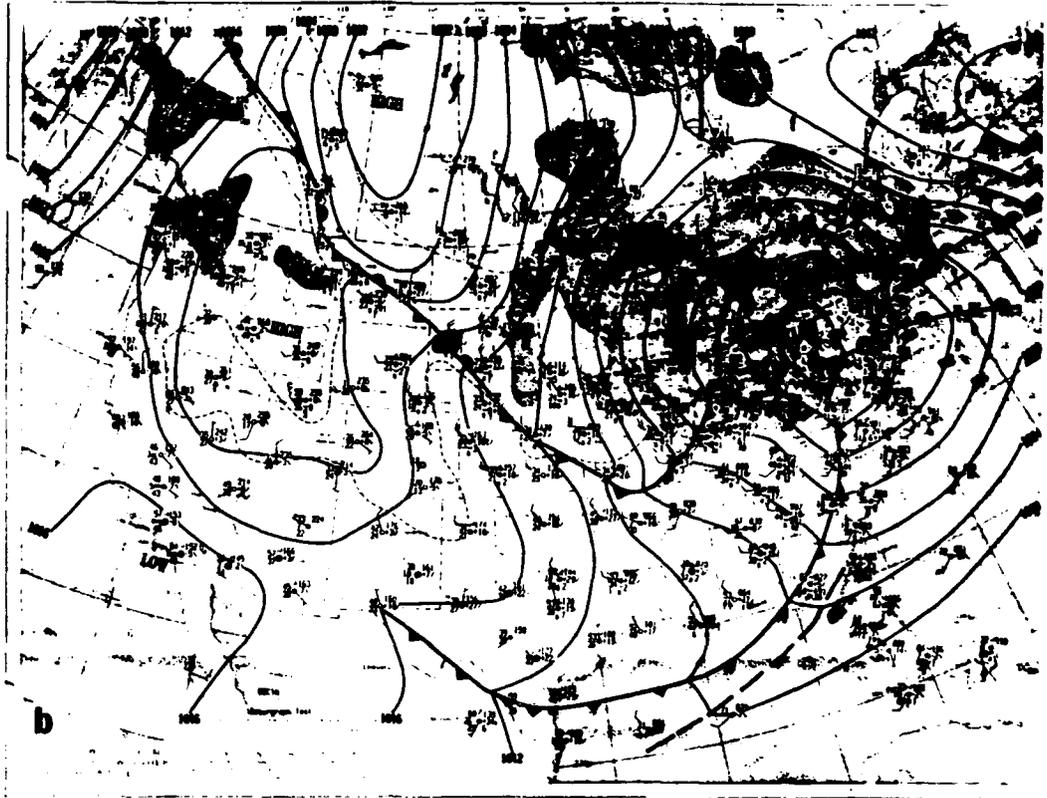
Figure 4-14. b) Surface chart for 12 UTC 14 Feb 91. Solid lines depict sea level pressure (mb) and precipitation areas are shaded (NOAA, 1991). **c)** 1235 UTC 14 Feb 91 NWS National Radar Summary (NOAA, 1991).

By 15/00 UTC the storm became vertically stacked. The 300 mb winds continued to be strong with 75 m/s winds in the base of the trough (not shown). At 500 mb the winds had increased to 75 m/s in the base of the trough (not shown). On the

surface the storm assumed a classic occluded pattern, however the precipitation pattern was quite unorganized. By this time the storm began to fill as it moved into Canada (Fig. 4-1b).

4.4 SEAM Output: Normal Case

The normal storm begins in the center of the country (Fig. 4-11), avoiding problems with linear interpolation at the edge of the grid. The 13/12 UTC Sutcliffe term output (Fig. 4-15a) reveals a maximum center over western Illinois. This corresponds relatively well to the direction of movement over the next 12 hours. However, the storm did not move along the Sutcliffe value maximum as shown in the bomb case, but nearly perpendicular to the axis of maximum Sutcliffe value that runs from southwest Missouri to Lake Michigan. Unlike the early periods of the bomb case, with the exception of the heating term (Fig. 4-15e) which is small, the terms are relatively equal in order of magnitude (Figs. 4-15a-d).

The latent heating term in the normal case   clearly weak compared to the bomb case. Note that the radar summary for 13/1335 UTC (Fig. 4-12b) shows weak precipitation and virtually no strong convective storms. Relative magnitudes of terms for this time period are similar to the 15/12 UTC model output for the bomb case. At 15/12 UTC the bomb was beginning to weaken. In contrast, the normal storm (Fig. 4-1b) continues to develop, although development is weak and steady throughout the life

of the storm.

The Sutcliffe values at 13/12 UTC (Fig. 4-15a) are quite large compared to those for the bomb case at the beginning of the case study (Fig. 4-8a). Perhaps the large values at the edge of the grid on Fig. 4-8a are distorting the analysis. Note that small Sutcliffe values existed prior to rapid development in the bomb case, while large Sutcliffe values early in the development of the normal case. This reinforces the fact that Petterssen (1956) emphasized the configuration of terms and not their magnitude with regard to importance in contributing to development.

By 14/00 UTC the Sutcliffe values (Fig. 4-16) show a maximum north of the surface center (Indiana) with positive values downstream from the storm center toward the north and east. This does fit reasonably well with the future movement of the storm. The thickness and stability terms dominate this period with the storm center in an area of negative values of the heating term.

As the storm continues to the Northeast the Sutcliffe values at 14/12 UTC (Fig. 4-17) are weak and indistinct, although continuing to be positive at the surface storm center in western Pennsylvania. Note the lack of clearly defined couplets near or downstream from the storm on the Sutcliffe chart. In addition, any well defined features on the other charts are well behind the storm center in Illinois and North Carolina. This is clearly a contrast to the bomb case which had positive and negative couplets associated with the surface center throughout the life of the storm. The only exception in the bomb case to this is the stability term which in the latter time period of the bomb case did indeed show a maximum center well behind the storm (not shown).
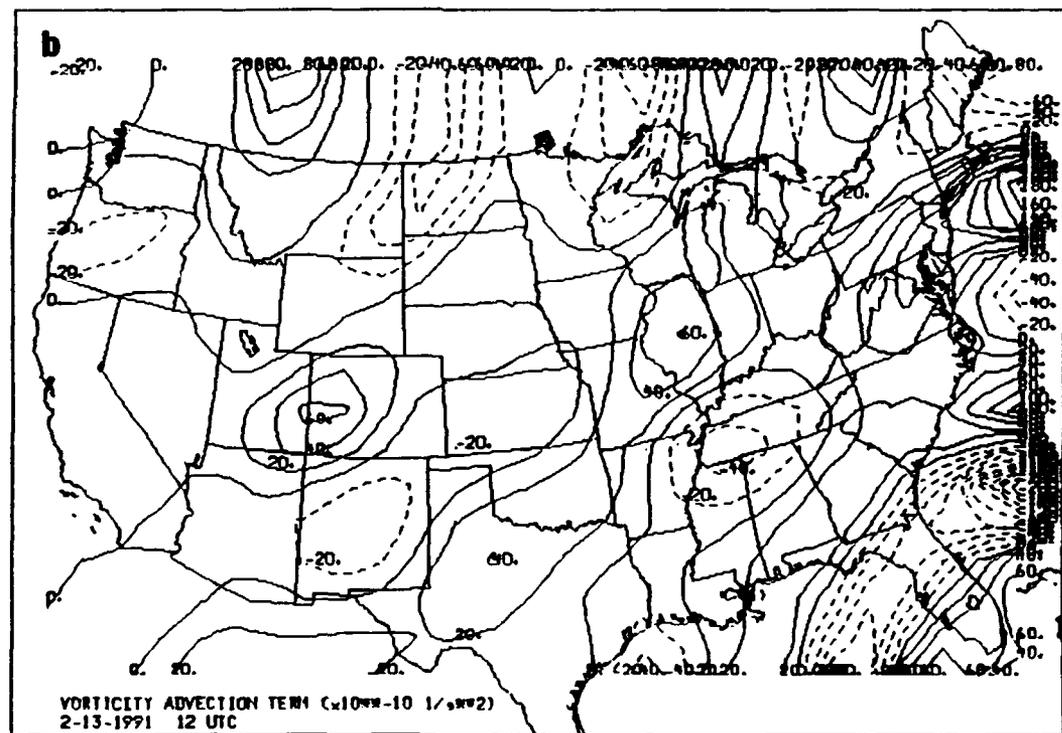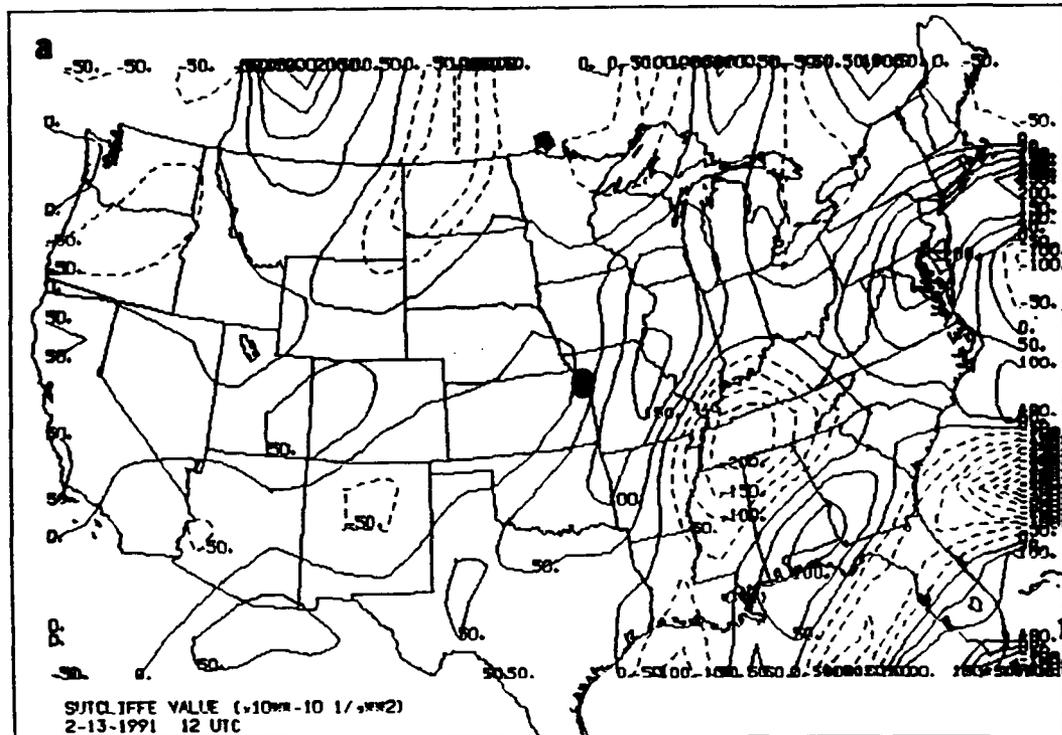
Figure 4-15. a) Sutcliffe Equation Analysis Model total values for 12 UTC 13 Feb 91 $(10^{-10} \, s^{-2})$. Dot is surface storm center. Solid lines are positive values and dashed lines are negative values. b) Vorticity Advection Term values for 12 UTC 13 Feb 91 $(10^{-10} \, s^{-2})$. Solid lines are positive values and dashed lines are negative values.
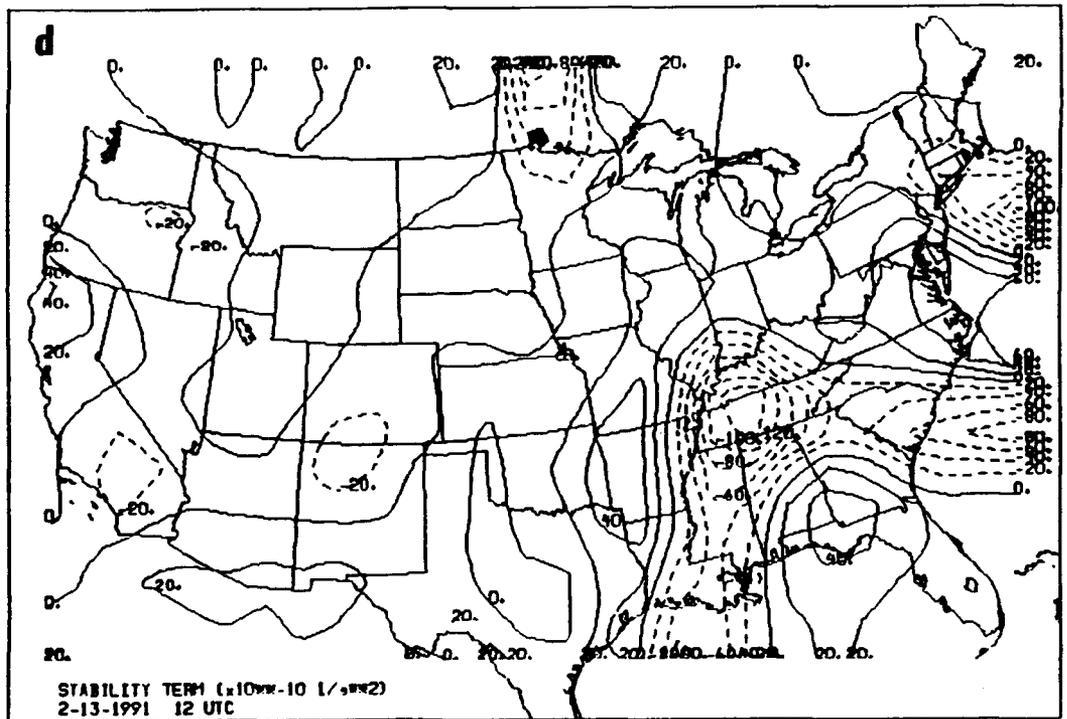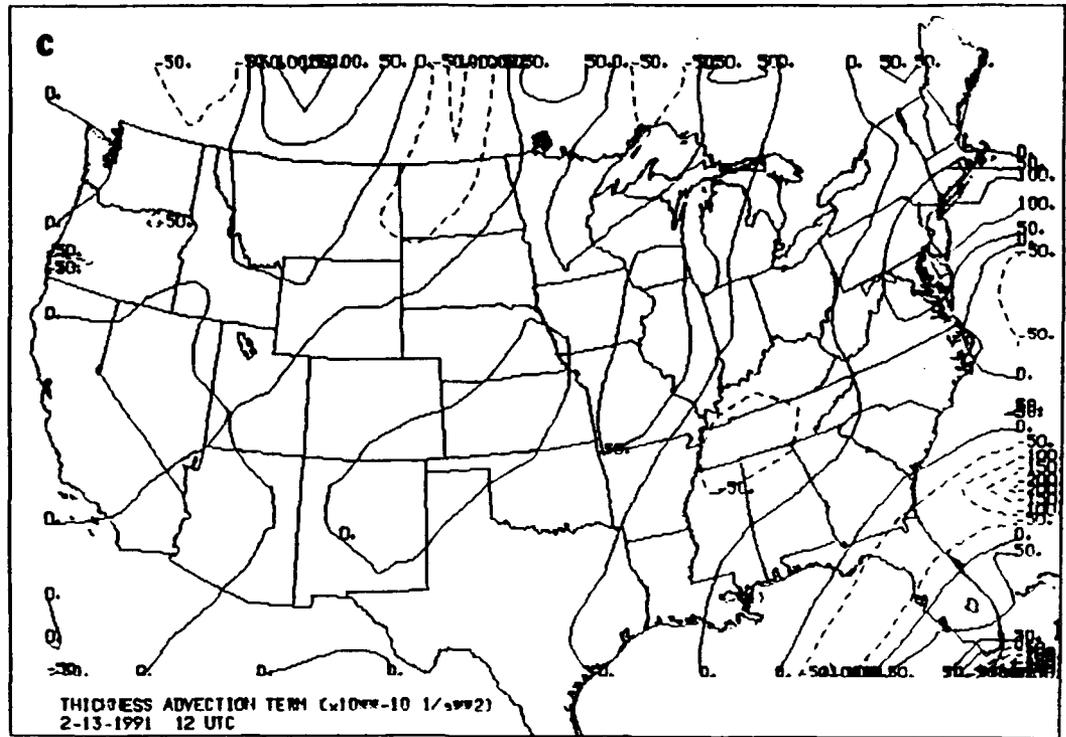
Figure 4-15. **c)** Thickness Advection Term values for 12 UTC 13 Feb 91 (10^{-10} s^{-2}). Solid lines are positive values and dashed lines are negative values. **d)** Stability Term values for 12 UTC 13 Feb 91 (10^{-10} s^{-2}). Solid lines are positive values and dashed lines are negative values.
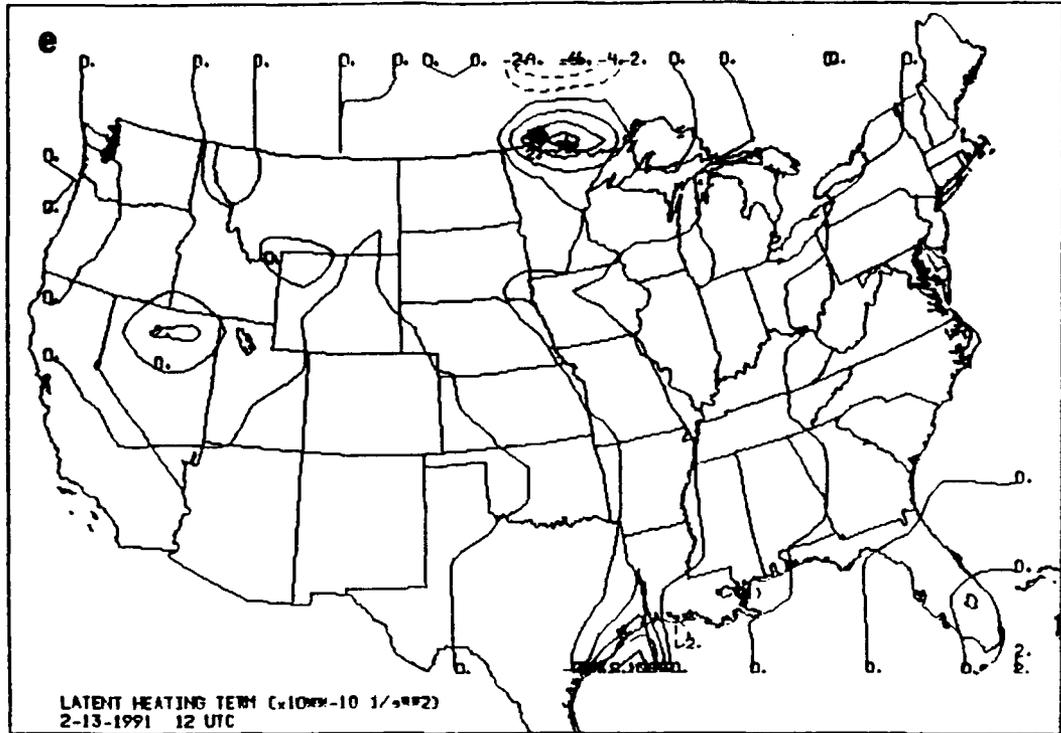
Figure 4-15e. Latent Heating Term values for 12 UTC 13 Feb 91 (10^{-10} s^{-2}). Solid lines are positive values and dashed lines are negative values.

For the final time period of the normal case, the output remains featureless. The 15/00 UTC Sutcliffe chart (Fig. 4-18) shows weak positive values at the storm center. Figure 4-1b shows the storm filling, one would expect negative Sutcliffe values.
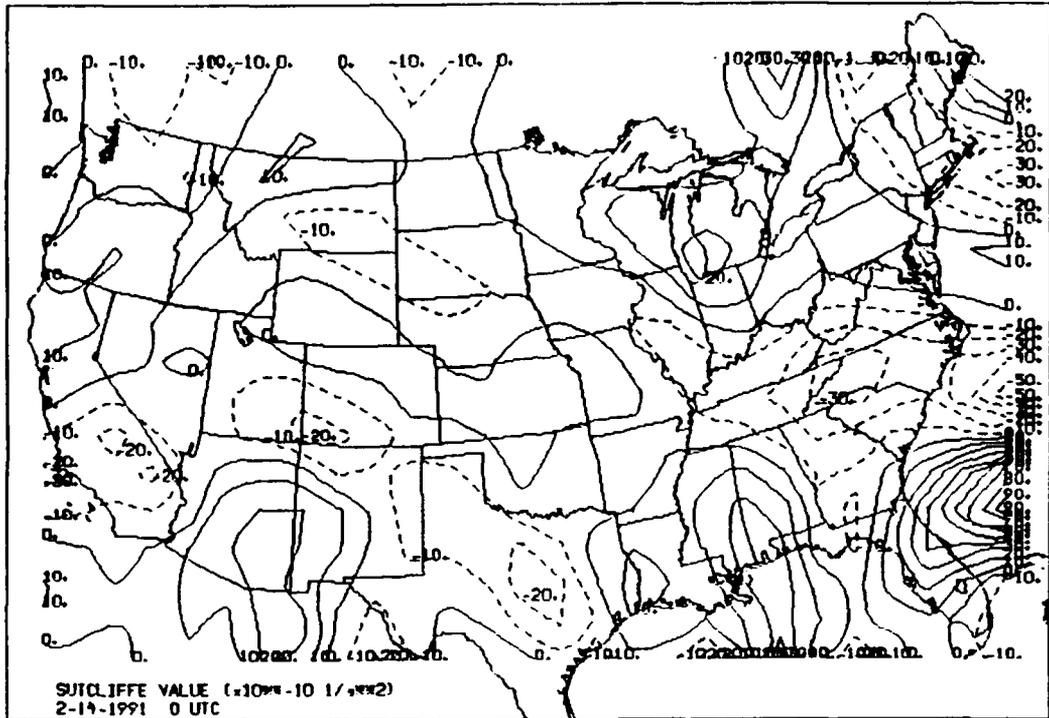
Figure 4-16. Sutcliffe Equation Analysis Model total values for 00 UTC 14 Feb 91 (10^{-10} s^{-2}). Dot is surface storm center. Solid lines are positive values and dashed lines are negative values.
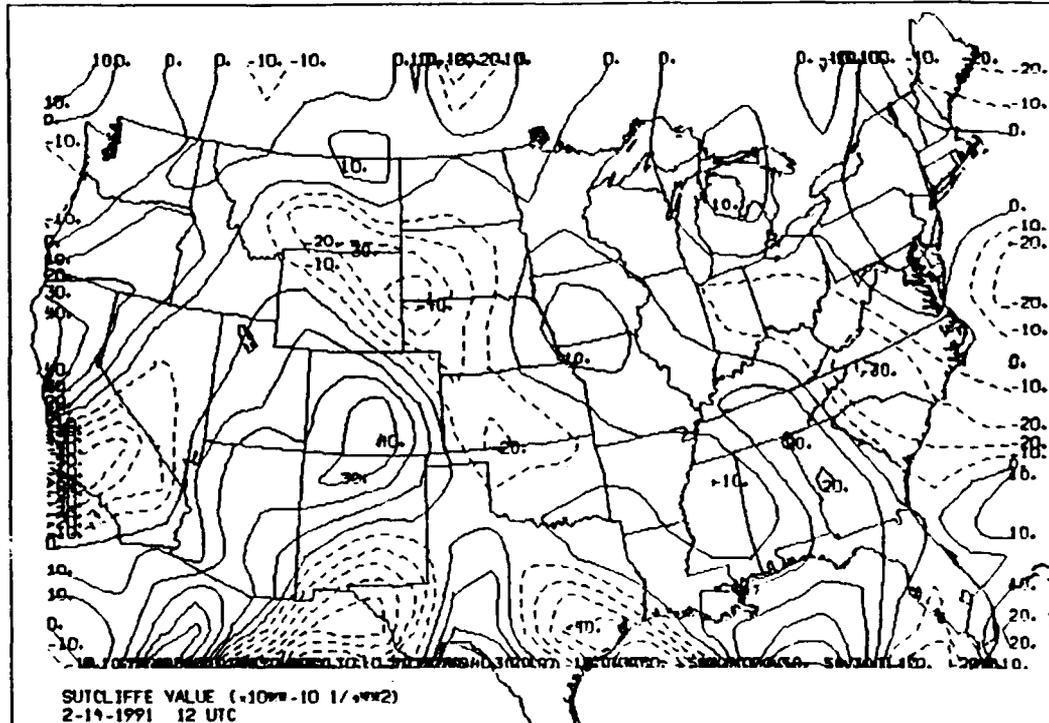
Figure 4-17. Sutcliffe Equation Analysis Model total values for 12 UTC 14 Feb 91 (10^{-10} s^{-2}). Dot is surface storm center. Solid lines are positive values and dashed lines are negative values.

60
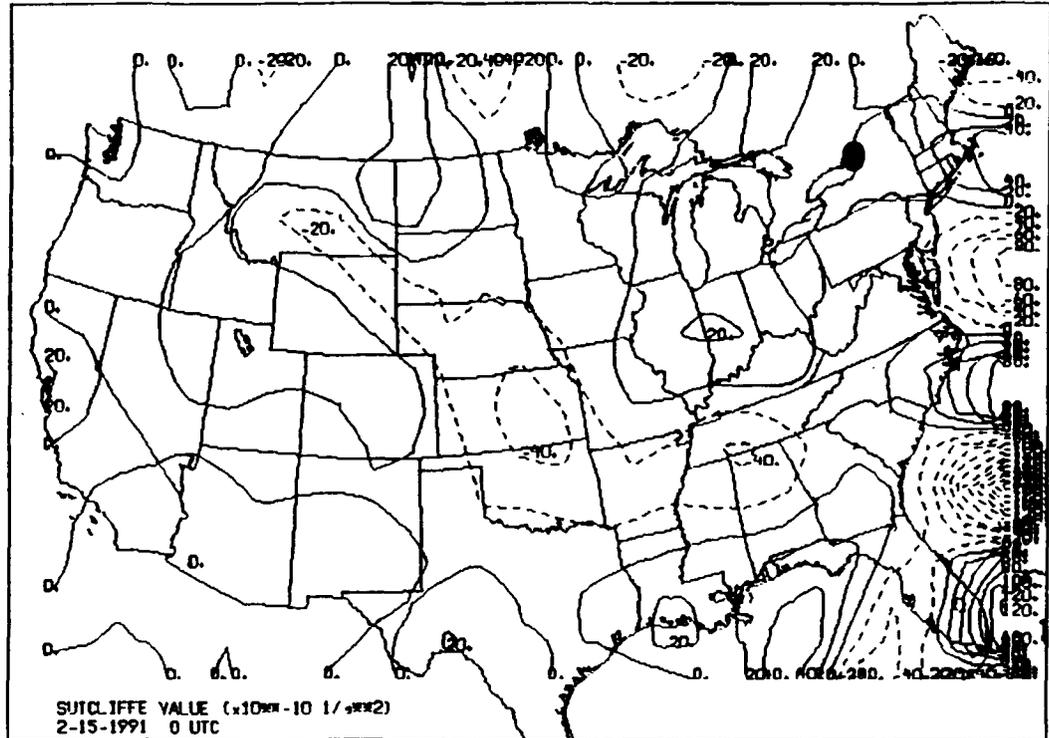
Figure 4-18. Sutcliffe Equation Analysis Model total values for 00 UTC 15 Feb 91 $(10^{-10}\ s^{-2})$. Dot is surface storm center. Solid lines are positive values and dashed lines are negative values.

Chapter 5: Summary and Conclusion

5.1 Summary of Model Results

Generally speaking, the model adequately analyzed the synoptic situation in both cases studied. In all time periods, except the final time period of the normal case, Sutcliffe values over the storm center were appropriate for the trend of the storm. In other words, if the storm was increasing in intensity the storm center Sutcliffe value was positive and vice versa.

The terms appeared to follow expected relative values as outlined in Petterssen (1956). It is difficult to assess the importance of the dominance of the different terms due to the limited number of cases. As previously discussed, it is commonly held that a synergism between the thickness, stability and heating terms is most important to the Sutcliffe development theory. Also, since the Laplacian is used, the shape of the field is of primary importance (Petterssen, 1956).

These two facts together lend significance to the configuration of the heating term at the 15/00 UTC time period for the bomb case. At 15/00 UTC, the initiation of explosive deepening (Fig. 4-1b), the heating term (Fig. 4-8e) had values on par with the thickness and stability terms. Also, the configuration of the heating term shows positive values clearly wrapped around the storm center. This pattern is unique to the bomb case and only at this key time period. In subsequent time periods values of the heating term drop off considerably. It also appears to correlate well with a twelve hour lag time between the latent heating maximum and the period of most rapid development. This fact agrees with statements of Smith, Dare, and Lin (1984) as well as Mac-

donald and Reiter (1988) which referred to latent heat release as a precursor to rapid development (see section 2.4).

In comparing convective to stable latent heating both favorable and conflicting results arise as compared to other authors findings as presented in section 2.4. Overall, SLHR values were much higher than those of CLHR. In fact, CLHR values were virtually non-existent in the normal case and the values in the bomb case were very small. However, this is generally supported by Macdonald and Reiter (1988) and Smith, Dare, and Lin (1984) who place an emphasis on stable rather than convective latent heating. The fact that CLHR values were so small could be a result of the difficulty in analysis due to the area averaging problem as previously noted (Smith and Tsou, 1985). Other possible explanations for small CLHR values include the lack of entrainment in the parameterization, the lack of surface data in the model, and the very restrictive criteria. These criteria include cloud base height, cloud thickness, convective instability, relative humidity threshold, vertical motion and integrated moisture convergence (see Appendix B). In consideration of the need for more accurate cumulus parameterization schemes as highlighted by Emanuel and Raymond (1992) and the findings of this research, continued work in this area is needed.

As previously discussed, the output from the SEAM must be viewed in light of the synoptic situation at hand. A prime example of this is the large Sutcliffe values in post frontal areas. Due to the fact that high stability term values appear behind the surface front these areas are not good indicators of development. Also, considering the synergistic effect of the terms, it is unlikely that one term could dominate the situation and provide useful results. Values of the individual terms must be considered in the interpretation of the Sutcliffe value. As more cases are explored, this area of concern

will naturally be addressed.

5.2 General Conclusions

Despite the fact that this study is a limited case comparison, some general conclusions can be drawn. After comparison of Sutcliffe values and storm tracks, it appears as though areas of positive Sutcliffe values downstream of the surface center indicate movement of the storm regardless of the nature of the storm. For the bomb case, the storm followed along the Sutcliffe value ridge, while the normal storm moved perpendicular to the ridge. This conclusion is preliminary of course, considering the degree of variability of storm tracks. The development trend of the storm is apparent as a result of the Sutcliffe value at storm center. Also, these preliminary results indicate that latent heat release is indeed important in rapid development. This conclusion is drawn from the relative lack of influence by the heating term in the normal case as compared to the dramatic influence seen in the bomb case. Actual importance of the configuration will require further study.

5.3 Areas for Future Research

Although this first version of the SEAM has proven to be a useful tool for analysis of cyclogenesis, there are many enhancements, both simple and complex, that could be implemented to enhance the further study of explosive and normal cyclogenesis. There are also other related areas that could be investigated to more clearly illuminate the role of latent heating in explosive cyclogenesis. The first step in this direction would be to extend this study beyond its limited case comparison to a statistically significant number of cases. In conjunction with the study of more cases, interpreta-

tion methods for the products of the SEAM and importance of various features, such as heating term configuration, can be developed.

Simple enhancements for the next iteration of the SEAM could allow for more detail and accuracy from the model. For simplicity, the model currently does not include surface data from upper air soundings or from the surface observation network. By adding this data, the base of the model could realistically deviate from the current uniform base of 1000 mb. Also, the influence of more accurate data in lower levels could have a significant impact on the analysis of cyclogenesis. In conjunction with this enhancement, the drag coefficient (C_D) could be varied based upon geographic properties near any particular grid point for a more accurate description of contribution of moisture from the surface.

There are other more involved ideas for future enhancement of the SEAM including the most complex portion of the model; cumulus parameterization. One possible way to better parameterize the release of convective latent heat release is to implement a finer mesh grid in areas of convection. This embedded mesoscale model would help alleviate the sub-grid scale problems associated with the cumulus parameterization. Implementing this enhancement would require a major overhaul of the SEAM in order to allow a limited area fine mesh grid to actually move through the larger grid in conjunction with the convection for each time period analyzed. Frank (1983) addressed the related issue of mesoscale vertical motions versus synoptic scale vertical motions. Implications are that this would require a separate and more detailed parameterization for mesoscale vertical motions in this embedded mesoscale model.

Another area of enhancement would be to calculate vertical profiles of signifi-

cant parameters as done previously by other authors (Lupo and Smith, 1992; Lin and Smith, 1979). These profiles could then be examined to provide further insight into the effects of these various factors at different levels throughout the atmosphere and their effect on cyclogenesis.

Stability has been discussed as a significant factor in the SEAM, and is vital to the amount of latent heating released, both stable and convective. The SEAM could be further enhanced by adopting the definitions of static stability as presented by Stull (1991). This could allow for increased accuracy in the amounts of latent heating allowed into the atmosphere for contribution to the cyclogenetic processes. In concert with this idea is to continue to examine different cumulus parameterization schemes as they become available. For example, Grell and Kuo (1991) reviewed eight different schemes and Frank (1983) examined the cumulus parameterization problem in a more general sense. Since cumulus parameterization is the most complex section of the SEAM, current views on the aspects of cumulus parameterization could continue to have an effect and should be put to the test when they become available. The author has made a serious attempt to keep the structure of the FORTRAN code modular to facilitate such changes and experiments. Portions of the SEAM source code are already being used by other graduate students at Saint Louis University as a result of this modularity. Due to the fact that (1) is a local time tendency equation, the SEAM could be used as a basis for a cyclogenesis forecast model as well. This would be similar to the methods applied by Lupo and Smith (1992).

5.4 Closing Remarks

The SEAM is designed to be a tool for analysis of cyclogenesis utilizing the Sut-

cliffe development theory. Future enhancements to this initial effort will provide for increased information from standard data sources concerning cyclogenesis in general and explosive cyclogenesis in particular. The first step in this process is to analyze more cases with this new tool. In addition, consideration must be given to the fact that the Sutcliffe Development Theory is restrictive, especially in that upper level influences are ignored. This initial research effort is a first step in analyzing the role latent heating plays in cyclogenesis. Current and near term versions of the SEAM must be used with the knowledge that only the lower layers (1000 mb to 500 mb) have an effect in these data analyses.

Appendix A: Symbols

The symbols are presented in the order of appearance in the text.

ζ_{1000}	relative vorticity at 1000 mb (s^{-1})
$\vec{V}$	wind velocity vector (ms^{-1})
η_{500}	absolute vorticity at 500 mb (s^{-1})
R_d	gas constant for dry air ($287 \ JK^{-1}kg^{-1}$)
f	Coriolis parameter (s^{-1})
∇^2	Laplacian operator
$\Delta\Phi$	Geopotential thickness
ω	vertical motion (ms^{-1})
ρ	density (kgm^{-3})
g	acceleration due to gravity ($9.806 \ ms^{-2}$)
Γ_D	dry adiabatic lapse rate ($0.0098 \ Km^{-1}$)
γ	environmental lapse rate (Km^{-1})
c_p	specific heat of air at constant pressure ($1004. \ JK^{-1}kg^{-1}$)
Q	latent heating (Jkg^{-1})
u_g	u-component of the geostrophic wind (ms^{-1})
Φ	geopotential
v_g	v-component of the geostrophic wind (ms^{-1})
η_g	absolute geostrophic vorticity (s^{-1})
ζ_g	relative geostrophic vorticity (s^{-1})
$\bar{u}$	average u-component of the wind from 1000 mb to 500 mb
$\bar{v}$	average v-component of the wind from 1000 mb to 500 mb
δ	distance between grid points (190.5 km)

F	generic representation of a field of values
S_d	static stability in dry conditions (KPa^{-1})
T_v	virtual temperature (K)
Θ_v	virtual potential temperature (K)
T_e	equivalent temperature (K)
Θ_e	equivalent potential temperature (K)
RH	relative humidity
S_b	static stability in moist conditions (KPa^{-1})
S_a	adjusted static stability (KPa^{-1})
p	pressure (mb, Pa)
$SLHR$	stable latent heat release (Ks^{-1})
L	latent heat (Jkg^{-1})
q_s	saturation mixing ratio (gkg^{-1})
$CLHR$	convective latent heat release (Ks^{-1})
b	moisture convergence availability parameter
M_t	integrated moisture convergence (kgm^{-2}s^{-1})
T_c	convective temperature (C)
T	temperature (C)
Θ	potential temperature (K)
p_b	pressure at the base of the cloud or layer (Pa)
p_t	pressure at the top of the cloud or layer (Pa)
C_d	Cressman drag coefficient (2.0x10^{-3})
ρ_b	density at the base of the cloud or layer (kgm^{-3})

$\nabla \cdot \vec{V} q$ moisture divergence (s^{-1})

$\vec{V}_b$ wind vector at the base of the cloud or layer (ms^{-1})

q_s mixing ratio at the surface (gkg^{-1})

q_b mixing ratio at the base of the cloud or layer (gkg^{-1})

Appendix B: Convective Latent Heating Flowchart
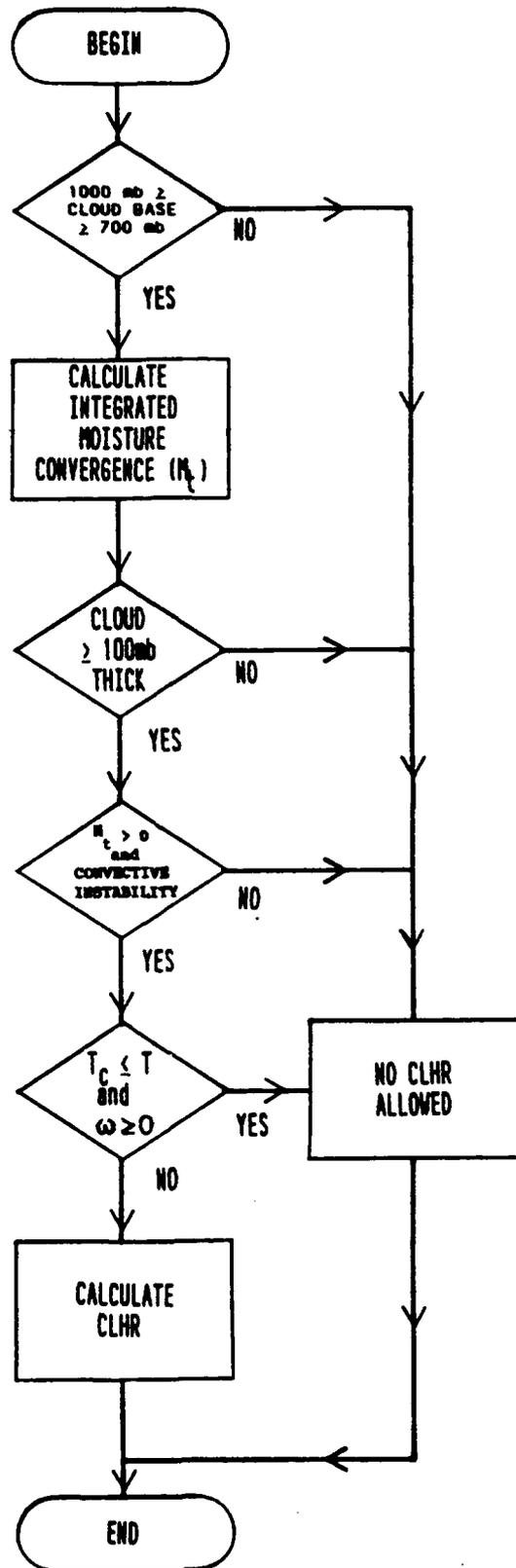
Bibliography

Adams, Michael E., 1989: Anatomy of a "Bomb": Diagnostic Investigation of Explosive Cyclogenesis Over the Mid-West United States. M. S. Thesis, North Carolina State University, Raleigh NC, 102 pp.

Anthes, R. A., 1977: A cumulus parameterization scheme utilizing a one-dimensional cloud model. *Monthly Weather Review, 105,* 270-286.

Barnes, Stanley L., 1973: Mesoscale Objective Map Analysis Using Weighted Time-series Observations. NOAA Technical Memorandum ERL NSSL-62, Norman, OK, 60 pp.

Cressman, G. P., 1960: Improved terrain effects in barotropic forecasts. *Monthly Weather Review, 88,* 327-342.

Dare, Patricia M., Phillip J. Smith and John T. Shively, 1985: The Role of Convective and Stable Latent Heat Release in the Development of an Extratropical Cyclone. *Preprints, Seventh Conference on Numerical Weather Prediction,* Montreal, Canada, American Meteorological Society, 232-236.

Doswell, Charles A. III, Joseph T. Schaefer and Donald W. McCann, 1982: Thermodynamic Analysis Procedures at the National Severe Storms Forecast Center. *Preprints of the Ninth Conference on Weather Forecasting & Analysis,* 304-309.

Edmon, Harold J. and Dayton G. Vincent, 1976: An Application of Two Tropical Parameterization Schemes of Convective Latent Heat Release in Middle Latitudes. *Monthly Weather Review, 104,* 1141-1153.

Emanuel, K. A. and D. J. Raymond, 1992: Report from a Workshop on Cumulus Parameterization, Key Biscayne, Florida, 3 - 5 May 1991, *Bulletin of the American Meteorological Society, 73,* 318-325.

Frank, William M., 1983: Review: The Cumulus Parameterization Problem. *Monthly Weather Review, 111,* 1859-1871.

Grell, Georg A. and Ying-Hwa Kuo, 1991: Semiprognostic Tests of Cumulus Parameterization Schemes in the Middle Latitudes. *Monthly Weather Review, 119,* 5-31.

Haltiner, George J. and Roger Terry Williams, 1980: Numerical Prediction and Dynamic Meteorology, John Wiley and Sons, Inc., New York, NY, 477 pp.

Hess, Seymour L., 1959: Introduction to Theoretical Meteorology, Robert E. Krieger Publishing Company, Malabar, FL, 364 pp.

Hirschberg, Paul A. and J. Michael Fritsch, 1991: Tropopause Undulations and the Development of Extratropical Cyclones. Part II: Diagnostic Analysis and Conceptual Model. *Monthly Weather Review, 119,* 518-550.

Kocin, P. J. and L. W. Uccellini, 1990: Snowstorms Along the Northeastern Coast of the United States: 1955 to 1985, American Meteorological Society, Boston, MA, 280 pp.

Krishnamurti, T. N., M. Kanamitsu, B. F. Ceselski and M. B. Mather, 1973: Florida State University's tropical prediction model. *Tellus, 25,* 523-535.

___ and Walter J. Moxim, 1971: On Parameterization of Convective and Nonconvective Latent Heat Release. *Journal of Applied Meteorology, 10,* 3-13.

Kuo, H. L., 1965: On Formation and Intensification of Tropical Cyclones Through Latent Heat Release by Cumulus Convection. *Journal of the Atmospheric Sciences, 22,* 40-63.

___, 1974: Further Studies of the Parameterization of the Influence of Cumulus Convection on Large-Scale Flow. *Journal of the Atmospheric Sciences, 31,* 1232-1240.

Li, Song Chin and Phillip J. Smith, 1979: Diabatic Heating and Generation of Available Potential Energy in a Tornado-Producing Extratropical Cyclone. *Monthly Weather Review, 107,* 1169-1183.

Lupo, Anthony R. and Phillip J. Smith, 1992: A comparison of synoptic-scale development characteristics for over-water and over-land cases of explosive cyclone development. *AMS Preprints - Symposium on Weather Forecasting.* Atlanta, Georgia, January 5-10, 1992.

Macdonald, Bruce C. and Elmar R. Reiter, 1988: Explosive Cyclogenesis over the Eastern United States. *Monthly Weather Review, 116,* 1568-1586.

Manabe, S., 1956: On the Contribution of Heat Released by Condensation to the Change in Pressure Pattern. *Journal of the Meteorological Society of Japan, 31,* 308-320.

Moore, James T., Isentropic Analysis and Interpretation: Operational Applications to Synoptic and Mesoscale Forecast Problems, AWS/TN-87/002, August 1987.

NOAA, 1991: Daily Weather Maps, Weekly Series February 11-17, 1991, U. S. Department of Commerce / NOAA / Climate Analysis Center.

O'Brien, James J., 1970: Alternative Solutions to the Classical Vertical Velocity Problem. *Journal of Applied Meteorology, 9,* 197-203.

Petterssen, S., 1956: Weather Analysis and Forecasting, Volume I: Motion and Motion Systems, McGraw-Hill Book Co., New York, NY, 428 pp.

Rao, Gandikota V. and Alan W. Hassebrock, 1972: Mesoscale Latent Heat Release and Its Influence on Mid-Tropospheric Warming. *Journal of Applied Meteorology, 11,* 1271-1283.

Reed, Richard J., Adrian J. Simmons, Mark D. Albright and Per Unden, 1988: The Role of Latent Heat Release in Explosive Cyclogenesis: Three Examples Based on ECMWF Operational Forecasts. *Weather and Forecasting, 3,* 217-229.

Roebber, Paul J., 1984: Statistical Analysis and Updated Climatology of Explosive Cyclones. *Monthly Weather Review, 112,* 1577-1589.

___, 1989: On the Statistical Analysis of Cyclone Deepening Rates. *Monthly Weather Review, 117,* 2293-2298.

Sanders, Frederick, 1987: Skill of NMC Operational Dynamic Models in Prediction of Explosive Cyclogenesis. *Weather and Forecasting, 2,* 322-336.

___ and John R. Gyakum, 1980: Synoptic-Dynamic Climatology of the "Bomb". *Monthly Weather Review, 108,* 1589-1606.

Schaefer, Joseph T., 1977: An Improved Second Order Finite Difference Analogue for the Laplacian Operator. *Journal of the Meteorological Society of Japan, 55,* 511-517.

Smith, Phillip J., Patricia M. Dare and Shiang-Jiun Lin, 1984: The Impact of Latent Heat Release on Synoptic-Scale Vertical Motions and the Development of an Extratropical Cyclone System. *Monthly Weather Review, 112,* 2421-2430.

___ and Chao Ping Lin, 1978: A Comparison of Synoptic-Scale Vertical Motions Computed by the Kinematic Method and Two Forms of the Omega Equation. *Monthly Weather Review, 106,* 1687-1694.

___ and Chih-Hua Tsou, 1985: Adiabatic and Diabatic Forcing of the Development of a Winter Extratropical Cyclone. *Preprints, Seventh Conference on Numerical Weather Prediction,* Montreal, Canada, American Meteorological Society, 219-225.

Storm Data, December 1987, Volume 29, Number 12, U. S. Department of Commerce / NOAA / NESDIS / National Climatic Data Center, Asheville, NC.

Stull, Roland B., 1991: Static Stability -- An Update. *Bulletin of the American Meteorology Society, 72,* 1521-1529.

Sutcliffe, R. C., 1939: Cyclonic and Anticyclonic Development. *Quarterly Journal of the Royal Meteorological Society, 65,* 518-524.

___, 1947: A Contribution to the Problem of Development. *Quarterly Journal of the Royal Meteorological Society, 73,* 370-383.

___ and A. G. Forsdyke, 1950: The Theory and Use of Upper Air Thickness Patterns in Forecasting. *Quarterly Journal of the Royal Meteorological Society, 76,* 189-217.

Uccellini, Louis W., 1988: Processes Contributing to the Rapid Development of Extratropical Cyclones. *Preprints, Palmen Memorial Symposium on Extratropical Cyclones,* Helsinki, Finland, American Meteorological Society, 110-115.

Wallace, John M., and Peter V. Hobbs, 1977: <u>Atmospheric Science</u>, Academic Press, Inc., New York, NY, 467 pp.

Biography of the Author

Donald Matthew Rinderknecht was born on December 19, 1960 in Cedar Rapids, Iowa. He graduated from Blaine Senior High School, Blaine, Minnesota in 1979. He enlisted in the US Air Force in 1980 and began work as a weather observer at Griffiss AFB, Rome, New York. In 1982, he was released from active duty under the Airman Scholarship Commissioning Program to pursue his Bachelor of Science in meteorology. The University of Wisconsin - Madison conferred his degree in May of 1986. Returning to active duty in the Air Force, he was assigned to Scott AFB where he worked at the USAF Environmental Technical Applications Center and the base weather station. He then went to Osan AB, Republic of Korea to serve as a Wing Weather Officer, after which, he entered the Air Force Institute of Technology program to earn a Master of Science (Research) degree in meteorology from Saint Louis University, Saint Louis, Missouri. He has since been assigned to instructor duty at Chanute AFB, Illinois where he is instructing Air Force personnel on satellite meteorology, environmental support for electro-optical weapon systems, doppler radar operations and interpretation, severe weather, and atmospheric physics. He is married to the former Penney Madeline Chapin of South Pasadena, California.